

Covalent Inhibitors of Interleukin-2 Inducible T Cell Kinase (Itk) with Nanomolar Potency in a Whole-Blood Assay

Christoph W. Zapf,^{*,†} Brian S. Gerstenberger,[‡] Li Xing,[†] David C. Limburg,[‡] David R. Anderson,[‡] Nicole Caspers,[§] Seungil Han,[§] Ann Aulabaugh,[§] Ravi Kurumbail,[§] Subarna Shakya,^{||} Xin Li,^{||} Vikki Spaulding,^{||} Robert M. Czerwinski,^{||} Nilufer Seth,^{||} and Quintus G. Medley^{||}

[†]BioTherapeutics Chemistry, Pfizer Worldwide Medicinal Chemistry, 200 Cambridgepark Drive, Cambridge, Massachusetts 02140, United States

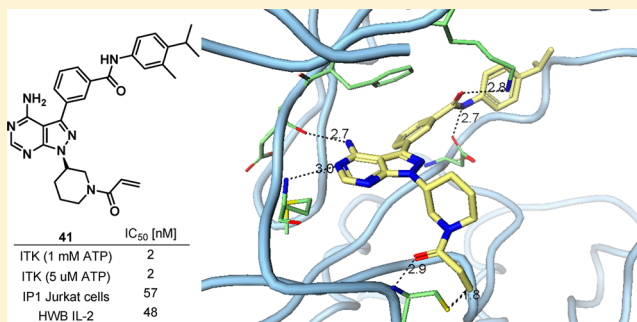
[‡]BioTherapeutics Chemistry, Pfizer Worldwide Medicinal Chemistry, Eastern Point Road, Groton, Connecticut 06340, United States

[§]Structure Biology and Biophysics, Pfizer Worldwide Medicinal Chemistry, Eastern Point Road, Groton, Connecticut 06340, United States

^{||}Inflammation and Autoimmunity, Pfizer Research, 200 Cambridgepark Drive, Cambridge, Massachusetts 02140, United States

S Supporting Information

ABSTRACT: We wish to report a strategy that targets interleukin-2 inducible T cell kinase (Itk) with covalent inhibitors. Thus far, covalent inhibition of Itk has not been disclosed in the literature. Structure-based drug design was utilized to achieve low nanomolar potency of the disclosed series even at high ATP concentrations. Kinetic measurements confirmed an irreversible binding mode with off-rate half-lives exceeding 24 h and moderate on-rates. The analogues are highly potent in a cellular IP1 assay as well as in a human whole-blood (hWB) assay. Despite a half-life of approximately 2 h in resting primary T cells, the covalent inhibition of Itk resulted in functional silencing of the TCR pathway for more than 24 h. This prolonged effect indicates that covalent inhibition is a viable strategy to target the inactivation of Itk.



■ INTRODUCTION

The nonreceptor tyrosine kinase Itk (interleukin-2 inducible T-cell kinase) is a member of the TEC-kinase family which encompasses Itk, Rlk, Btk, Bmx, and Tec. It is expressed mainly in immune cells such as T cells, mast cells, NK cells, and NKT cells. Recent work suggests that Itk may be a negative regulator in mast cells as responses of mast cells lacking Itk to FcεR1 signaling are not attenuated and can be increased relative to WT mast cells.¹ In contrast, Itk positively regulates T cell receptor (TCR) signaling and plays a role in numerous T cell responses.² Itk is activated downstream of the T cell receptor and activates PLCγ1 by phosphorylation. This leads to the production of IP3 and DAG and triggers the release of intracellular calcium and activation of PKCβ, respectively. These actions induce T cell proliferation and drive transcription of cytokines through NFATc.^{2–4} For an excellent and more comprehensive schematic representation of the TCR pathway please refer to the recent literature.²

Itk is strongly upregulated upon activation of naive T cells, and both respond to and drive the expression of IL-2. It is the sole TEC kinase expressed in Th2 T cells and has been shown to play a key role in Th2 cytokine production *in vivo*.^{5–7} Itk has also been implicated in the production of IL-17A in Th17 cells.⁸ An effect on T cell integrins has been shown to involve

Itk and can alter binding to APC's and the extracellular matrix.^{2–4} In addition to its role in the TCR pathway, Itk has been shown to be involved in the response of T cells to several chemokines, and Itk knockout T cells have reduced chemotaxis to SDF-α1.^{5,9,10} Itk KO mice also have reduced T cell recruitment to the lungs in OVA-asthma models, suggesting a role for Itk in T cell trafficking. Additionally, the use of RNA interference studies, kinase-inactive Itk mutants, and Itk small molecule inhibitors demonstrated that efficient uptake of HIV by CD4 + T cells and viral replication requires Itk kinase activity.¹¹

Several potent ATP-competitive small-molecule Itk inhibitors have been reported in the literature to date (Figure 1). BMS disclosed some of the earliest potent and selective small molecule Itk inhibitors¹² focusing on aminothiazoles such as compound 1.¹³ Subsequently, Boehringer Ingelheim disclosed several papers^{14–18} culminating in the discovery of highly optimized benzimidazoles such as analogue 2.¹⁹ Very recently, Vertex published their own SAR efforts around the potent pyridone template (3)²⁰ and a detailed understanding of the hydration state of the Itk active site.²¹ Mannkind and GSK also disclosed several potent Itk

Received: August 13, 2012

Published: October 25, 2012

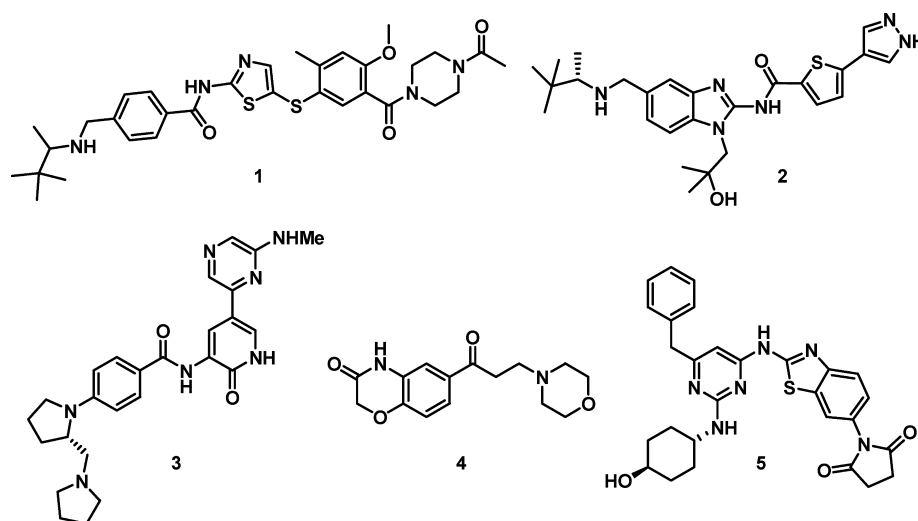


Figure 1. Known Itk inhibitors from the literature.

inhibitors represented by aryl ketone **4**²² and aminobenzothiazole **5**,^{23,24} respectively.

Despite these advances, to the best of our knowledge no Itk inhibitors have been advanced to clinical trials. It should be pointed out that literature reported inhibition values were generally determined in the presence of ATP concentrations corresponding to the K_m of the enzyme ($\sim 5 \mu\text{M}$). When tested in a cellular environment with an ATP concentration of 1–2 mM, ATP-competitive inhibitors were found to be 30–50-fold less potent as predicted by Cheng-Prusoff.²⁵ To overcome this problem of biochemical efficiency, other modes of inhibition need to be applied.²⁶

Non-ATP-competitive kinase inhibition is an approach that is getting increased attention because this strategy allows improved selectivity.^{27,28} A recently disclosed allosteric site on Itk²⁹ drove a discovery program targeting small molecule allosteric inhibitors of Itk.³⁰

A recent analysis of the marketed drugs highlights that more than half of them undergo a chemical reaction in the enzyme's active site or are structurally related to the natural substrate.³¹ In spite of the pharmaceutical industry's tendency to shy away from deliberately targeting covalent inhibitors, this class of compounds is experiencing renewed interest presumably due to some of the inherent mechanistic advantages.³² Much effort has been brought forth to understand the relationship between the reactivity of an electrophile and its potential toxicological profile in order to predict and derisk off-target reactivity.³³ More than half of the 39 FDA approved covalent drugs are utilized either as antibiotics or anticancer medicines. However, one cannot ignore the fact that in 2010 two of the top five selling drugs in the US were known to be covalent inhibitors (Nexium and Plavix) and did not belong to either drug class.³²

Pfizer recently disclosed a series of inhibitors targeting Bruton's tyrosine kinase (Btk) in a covalent fashion.³⁴ The known covalent Btk inhibitor PCI32765,³⁵ which was advanced to clinical trials for the treatment of chronic lymphocytic leukemia and B cell lymphoma has also been reported to be a potent inhibitor of Itk.³⁶

Encouraged by these recent successful clinical applications of covalent inhibitors and with our institutional knowledge of advancing covalent inhibitors to clinical trials,³⁷ we initiated a program to target low dose³⁸ covalent inhibitors of Itk to overcome the biochemical efficiency hurdle inherent to the kinase. At the outset of this approach, concerns were considered with respect to selectivity over other cysteine containing kinases. Analysis

of the ATP binding site of 434 kinases revealed that 10 other kinases such as Btk, Egfr, Rlk, Jak3, etc. contain a cysteine corresponding to Cys442 in Itk, the cysteine to be targeted for covalent modification.

The microenvironment of Cys442 in Itk was perceived as an additional hurdle to discovering covalent Itk inhibitors. The pK_a of a cysteine sulfhydryl group can potentially be influenced in a substantial manner depending on the surrounding amino acids, leading to a wide range of reactivity. When comparing the cysteine-containing kinases, different pK_a -modifying amino acids can be found at the +3 position with respect to the cysteine. The majority of the cysteine-containing kinases in question either contain an Asp or an Asn in this position. Compared to the kinases displaying an Asn, the former amino acids lead to an increase in pK_a and concomitant reduction in nucleophilicity. Itk is characterized by the presence of Asp445, which leads to an increase in the pK_a of the cysteine to about 8.5, whereas Btk contains an Asn in the corresponding position resulting in a pK_a of about 7.7 for the respective cysteine. The expected reduction in nucleophilicity of Cys442 was perceived as an additional obstacle to discover a covalent inhibitor for Itk.

■ ITK HALF-LIFE DETERMINATION

To implement a successful covalent strategy for the inhibition of Itk, it was important to understand the stability of the inhibitor–Itk complex and the resynthesis rate or half-life of the kinase. To determine the half-life of Itk, human CD4⁺ T cells were used to perform a traditional pulse–chase experiment utilizing ³⁵S Met/Cys.³⁹ It was determined that Itk has a half-life of approximately one hour in resting primary CD4⁺ T cells (Figure 2) indicating that the protein is rapidly turned over in cells. We next tested if treatment of CD4⁺ T cells with covalent Itk inhibitors would affect Itk turnover. Cells were ³⁵S Met/Cys labeled and treated with a covalent inhibitor for 45 min. The cells were then washed to remove unbound inhibitor, and protein turnover was measured over time. It was demonstrated that treatment of cells with a covalent inhibitor stabilizes Itk leading to an increased half-life of 22 h.

To determine the pharmacodynamic effect of covalent Itk inhibition, T cells were stimulated at various times following covalent Itk inhibition, and the phosphorylation of PLC γ 1 was measured. Cells were treated with an Itk inhibitor for one hour

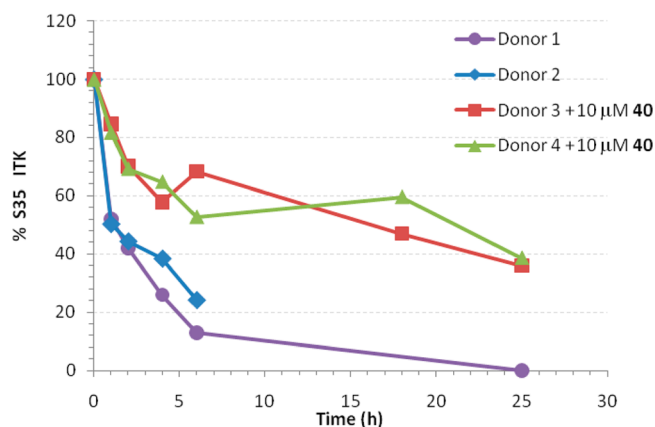


Figure 2. Pulse-chase experiment in the presence and absence of a covalent Itk inhibitor to determine the functional half-life of Itk in primary cells.

after which the excess inhibitor was removed by extensive washing, and the cells were cultured further. At different time points, cells were removed and activated through the TCR with anti-CD3/CD28 beads. The extent of phospho-PLC γ 1 was determined by SDS gel and Western blotting. Inhibition of the generation of phospho-PLC γ 1 lasted for up to 24 h following covalent Itk inhibition (Figure 3, data normalized to the absence

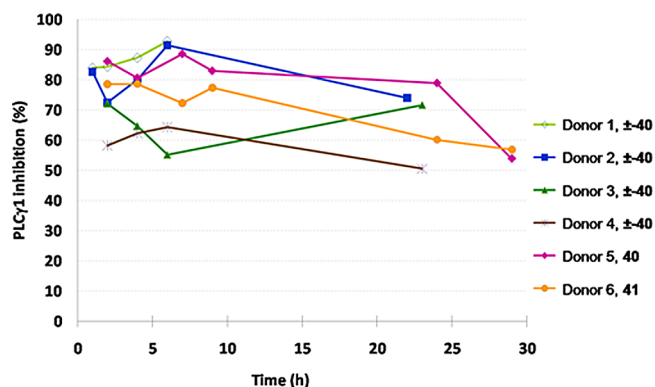


Figure 3. Determination of the inhibition of phospho-PLC γ 1 over time in the presence of 10 μ M covalent Itk inhibitors. The measured phospho-PLC γ 1 inhibition in the presence of an inhibitor was normalized to the control (absence of inhibitor).

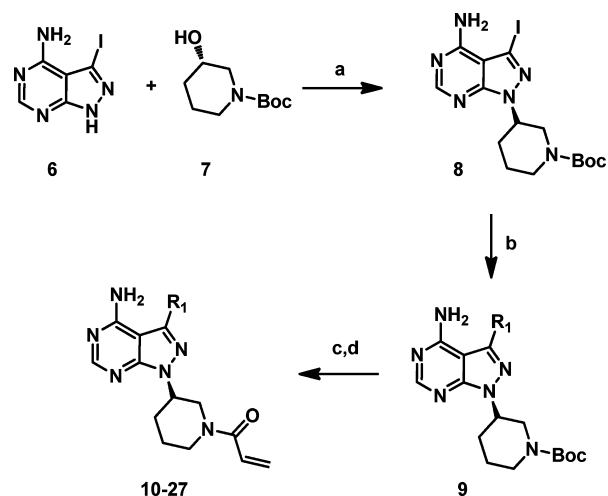
of the inhibitor). This prolonged pharmacodynamic effect following covalent Itk inhibition correlates well with the increased Itk half-life following the covalent inhibition that we observed. Phosphorylation has been linked to the regulation of protein turnover, and the cbl family of ubiquitin ligases are generally targeted to client proteins through a phosphorylation site.⁴⁰ It is possible that Itk autophosphorylation results in the formation of or regulates the formation of a ubiquitin–ligase binding site. Kinase activity has been linked to protein turnover in several signaling pathways including recent data showing that downstream Syk-dependent BCR signaling is required for BCR ubiquitination.⁴¹ Mice carrying a cbl-b E3 ubiquitin ligase-defective mutation have hyperactive TCR signaling and spontaneous autoimmunity showing that cbl family ubiquitin ligases play an important role in negative signaling in T cells.⁴²

CHEMISTRY

Syntheses of covalent pyrazolopyrimidines **10–27** commenced from reagent **6**³⁹ and commercially available **7** via a Mitsunobu

reaction to yield chiral iodopyrazolopyrimidine **8** in 70% yield (Scheme 1). This core could be elaborated by either applying

Scheme 1. Synthesis of Aryl and Heteroaryl-Substituted Pyrazolopyrimidines^a



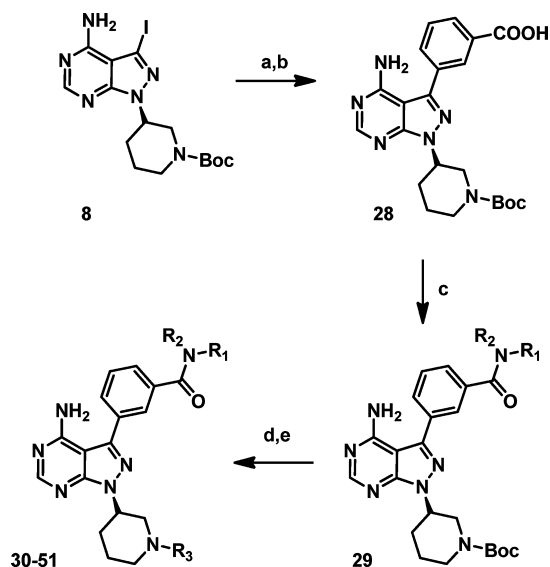
^aReagents and conditions: (a) DIAD, PPh₃, THF; (b) boronic acid, PdCl₂(dppf), K₂CO₃, 1,4-dioxane, 120 °C; (c) 4 N HCl, 1,4-dioxane; (d) EDCl, HOBT, TEA, acrylic acid, THF or acryloyl chloride, TEA, DCM.

parallel medicinal chemistry or singleton chemical synthesis. Suzuki couplings of iodide **8** to a variety of aryl and heteroaryl boronic acids provide piperidine **9** in moderate to good yield (60–70%). Subsequent Boc deprotection using 4 N HCl in dioxane cleanly provided the piperidine HCl salt in nearly quantitative yield. This salt could be used directly to install the acrylamide in **10–27** via amide coupling utilizing acrylic acid or via acryloyl chloride.

Synthesis of amide substituted pyrazolopyrimidines **30–51** used key intermediate **28** that was accessed via Suzuki coupling of iodide **8** followed by hydrolysis to provide acid **28** in 98% yield (Scheme 2). Direct access to benzoic acid **28** via Suzuki coupling with 3-boronobenzoic acid also provided the desired intermediate but was found to be problematic during scale up. Amide couplings using standard HATU conditions provided amides **29** in good to excellent yield (62–96%). Boc deprotection of **29** using 4 N HCl in dioxane again cleanly provided the piperidine HCl salt. As before, this salt could be used directly in the next step to install a variety of electrophiles via amide coupling conditions from the carboxylic acids or by utilizing acryloyl chloride to provide **30–51** in poor to moderate yield (8–61%). Intermediate **29** also reacted cleanly with cyanogen bromide to provide **64** (vide infra) in 55% yield.

RESULTS AND DISCUSSION

In an effort to explore novel chemical space, the corporate compound repository was surveyed for potentially covalent kinase inhibitors. Pyrazolopyrimidine **52** with an electrophilic acrylamide (Figure 4A) was found to be a potent Itk inhibitor in the enzyme assay in the presence of a physiological level of ATP (IC₅₀ = 73 nM). The compound was also tested in the IP1 assay in which Jurkat cells are treated with the inhibitor before anti-CD3 is added as a stimulus and the inhibition of PLC γ phosphorylation, the immediate downstream target of Itk, is measured. Compared to the enzyme assay, amide **52** was found

Scheme 2. Synthesis of Amide Substituted Pyrazolopyrimidines^a

^aReagents and conditions: (a) 3-(methoxycarbonyl)phenylboronic acid, PdCl₂(dppf), K₂CO₃, 1,4 dioxane, 120 °C; (b) NaOH, MeOH, H₂O; (c) HATU, TEA, HNR₁R₂, THF; (d) 4 N HCl, 1,4-dioxane; (e) HATU, TEA, R₃CO₂H, THF or R₃C(O)Cl, TEA, DCM or BrCN, Cs₂CO₃, DMF.

to display a substantial drop in potency in the cell assay (IC₅₀ = 2.21 μM). However, this *m*-amide analogue provided an intriguing starting point for further SAR exploration. An X-ray crystal structure of amide **52** (Figure 4B) revealed the compound's binding mode, which presumably allows the phenyl ring attached to the heterocyclic core to interact with the gatekeeper Phe435 through π -stacking. The crystal structure also confirmed that compound **52** engages Cys442 in a covalent bond between the β -carbon of the acrylamide and the cysteine sulfhydryl (C–S distance 2.0 Å). An additional hydrogen bond was detected between the carbonyl of the acrylamide and NH of the cysteine backbone (2.8 Å). The aminopyrimidine core interacts with Met438 and Glu436 at the hinge through two hydrogen bonds (3.1 and 2.8 Å). The π -stacking interaction of the phenyl ring attached to the pyrazolopyrimidine with gatekeeper Phe435

presumably positions the diarylamide group to form two hydrogen bonds with Lys391 (3.2 Å) and Asp500 (2.8 Å).

The crystal structure of **52** was compared to that of pyridone **3**,²⁰ which was recently disclosed by Vertex. The amino-pyrazine heterocycle in pyridone **3**, which was shown to interact with Lys391 and Glu406 via hydrogen bonds, overlaps reasonably well with the central phenyl ring in **52**. It was hypothesized that installation of a suitable heterocycle in place of the diaryl amide side chain in **52** could retain or improve potency while significantly reducing molecular weight. Furthermore, molecular modeling suggested that an aryl or heteroaryl side chain attached to the pyrazolo-pyrimidine heterocycle could potentially interact productively with the gatekeeper Phe435 by a π -stacking interaction.

The library of pyrazolopyrimidines **10–27** was prepared with the stereochemistry suggested by the crystal structure of acrylamide **52**. It was found that the π -stacking hypothesis was supported by the potencies of analogues **10–15** (Table 1), which correlate with the electronic nature of the phenyl rings. The electron-rich methoxy analogues **10** and **11** were more potent than the electron-deficient trifluoromethyl analogues **12** and **13**. The potency of the trifluoromethoxy analogues **14** and **15** were as expected. The *m*-substituted analogues in this set appeared to be slightly but consistently more potent than the corresponding *p*-substituted derivatives. Attempts to increase the electron density of the phenyl ring by addition of another alkoxy substituent did not lead to an improvement in potency (**16** and **17**) possibly due to steric interference. In contrast, benzyl alcohol derivative **18** did lead to a slight potency improvement as compared to the methoxy analogues.

Incorporation of a range of heterocyclic substituents attempting to engage Lys391 with or without an additional interaction to Glu406 did not provide the expected gain in potency as can be seen from analogues **19–24**. Likewise, attempting to form hydrogen bonds to sulfoxide **25** or sulfones **26** and **27** failed to improve the activity of the compounds. These aryl and heteroaryl-substituted pyrazolopyrimidines displayed an unsatisfying level of potency in the presence of a high ATP concentration. This finding led to the conclusion that the biaryl motif was an essential part of the pharmacophore.

Amide **52** was active in the enzyme assay, but its potency in the IP1 cell assay had to be improved. A library of amides was prepared for this purpose and to seek a replacement of the metabolically unfavorable *tert*-butyl group (Table 2). A broad

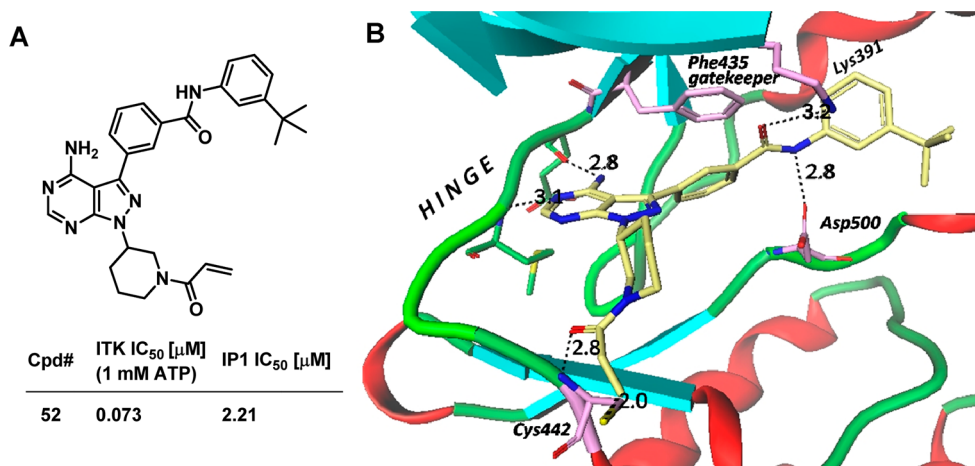
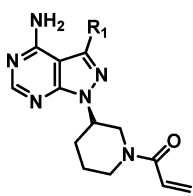


Figure 4. (A) Itk potency of amide **52**. (B) X-ray crystal structures of **52** in the ATP binding site of Itk (a portion of the P-loop was omitted for clarity purposes).

Table 1. Inhibition Constants of Aryl and Heteroaryl Substituted Pyrazolopyrimidines at Cellular ATP Concentration

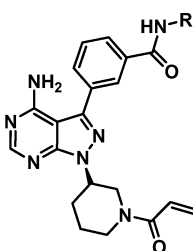


Cpd#	R ₁	IC ₅₀ [μ M] 1 mM ATP	Cpd#	R ₁	IC ₅₀ [μ M] 1 mM ATP
10		4.425	19		22.930
11		2.495	20		10.324
12		52.458	21		10.068
13		17.744	22		9.827
14		21.417	23		7.457
15		6.645	24		20.439
16		21.321	25		21.883
17		8.341	26		>100
18		1.045	27		>100

range of substituted anilines, benzylamines, phenethylamines, and alkylamines was explored varying the substitution pattern and electronic nature of the arene, while retaining the electrophilic acrylamide. Replacement of the *tert*-butyl group by a CF₃-group provided analogues 30 and 31, which are still potent but also showed a significant loss in activity compared to 52. The corresponding methoxy-analogues 32 and 33 were equipotent suggesting that the electronic nature of the distal arene does not influence the binding affinity. Other fluorophenyl derivatives 34–37 with varying substitution patterns did not provide an improvement in potency. Incorporation of a heteroatom to improve physical properties led to a potency loss for pyridines 38 and 39. A significant potency improvement compared to that of amide 52 was achieved with the *p*-isopropylphenyl analogues 40 and 41 (PF-06465469).⁴³

To probe the spatial tolerability of the pocket, the homologous benzyl and phenethylamines were tested. Similar to the *p*-isopropylphenyl analogues, the hydrophobic *tert*-butyl benzylamine derived amide 42 was found to be a highly potent covalent Itk inhibitor. While the CF₃-derived benzylamine analogue 43 shows the same level of potency compared to those of aniline-derived amides 30 and 31, the related benzylamides 44–47 and the phenethylamide 48 are substantially less potent. Alkylamine-derived

Table 2. Inhibition Constants of Amides at the Meta Position of a Phenyl Substituted Pyrazolopyrimidine at Cellular ATP Concentration



Cpd#	R ₁	IC ₅₀ [μ M] 1 mM ATP	Cpd#	R ₁	IC ₅₀ [μ M] 1 mM ATP
30		0.13	41		0.002
31		0.19	42		0.01
32		0.18	43		0.20
33		0.20	44		4.08
34		0.72	45		1.52
35		1.41	46		2.46
36		0.21	47		6.47
37		0.52	48		1.75
38		1.02	49		10.88
39		0.72	50		>100
40		0.01	51		36.22

amides such as 49–51 were either only weakly active or inactive. The series of compounds shown in Table 2 strongly suggests that an alkyl-substituted phenyl ring at the distal position of the covalent inhibitors is optimal for potency.

An additional feature of the crystal structure shown in Figure 4B is the stereochemistry of the piperidine ring. The presumed eutomer in this series is the (*R*)-enantiomer as shown. To confirm this finding, the (*R*)- and (*S*)-enantiomers 40 and 53 were prepared independently from chiral starting materials (Figure 5A), and the expected increase in potency was noted for the (*R*)-enantiomer in the three assays. Figure 5B illustrates the X-ray crystal structure of the two enantiomers. While both compounds form a covalent bond with the cysteine sulfhydryl, the (*R*)-enantiomer 40 is characterized by a hydrogen bond from the acrylamide carbonyl to the backbone protein, which cannot be detected in the structure of (*S*)-enantiomer. This additional

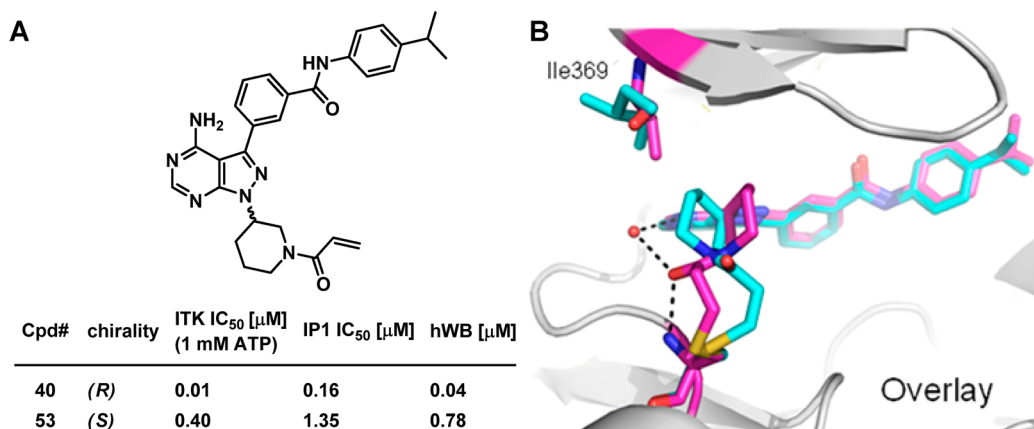


Figure 5. (A) Comparison of the potencies of the enantiomeric pair **40** and **53** highlights the critical influence of the stereogenic center. (B) Overlay of the two enantiomers bound to the ATP-binding site of Itk.

interaction provides improved potency for inhibitor **40**, which translates convincingly through the three assays.

As highlighted in Figure 4B, it was postulated that the amide bond between the aryl groups of analogue **52** forms a hydrogen bond with Lys391 and Asp500. To understand the contribution of engaging Asp500 in this interaction, methylated analogue **54** was prepared (Table 3). When tested in the inhibition assay, a

Table 3. Comparison of Amide **40** and **54** Demonstrates the Importance of the Amide's Hydrogen Bond Donor Function

compd #	R	Itk IC ₅₀ [μM] (1 mM ATP)
40	H	0.01
54	Me	>100

significant difference in potency was observed between the methylated and unmethylated analogue. Whereas the parent amide **40** is very potent in the enzyme assay at high ATP concentration (IC₅₀ = 10 nM), the corresponding N-methylated analogue **54** is essentially inactive, thus underscoring the critical nature of the engagement of this hydrogen bond.

Enantiomer **40** was subsequently utilized as a reference in a survey to explore the range of potential electrophiles that could be considered in subsequent covalent inhibitor designs. Table 4 highlights the analogues that were prepared for this comparison. While it appeared initially that any substitution around the acrylamide would be prohibitive (**55–57**), hydroxycrotonamide **58** and N-methylcrotonamide **59** clearly showed that the actual SAR is more complex. Further expansion of the electrophilic moiety initially led to an inactive piperazine analogue **60**. However, activity was restored upon extension of the polar functionality providing the elaborated analogue **61**. By increasing the electron density around the electrophile, the methyl substituents in **55–57** presumably lower the electrophilicity of the olefin. In comparison, the hydroxymethyl and N-methyl aminomethyl

Table 4. Comparing Various Covalent Warheads by Potencies and Calculated Electrophilicity

Cpd#	R	ITK IC ₅₀ [μM] (1 mM ATP)	IP1 IC ₅₀ [μM]	Electrophilicity ω [kcal/mol]
40		0.01	0.18	8.62
55		>100	NA	7.71
56		>100	NA	6.03
57		>100	NA	6.73
58		65	NA	8.62
59		7.57	NA	9.96
60		>100	NA	10.04
61		0.1	>50	8.23
62		0.01	0.07	8.78
63		>100	NA	7.41
64		>100	NA	1.89

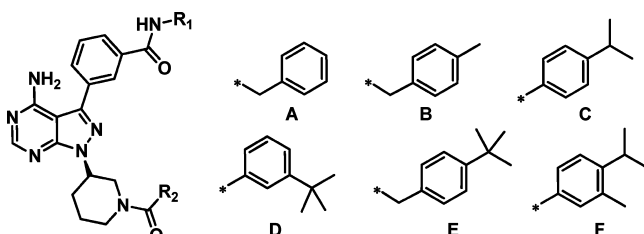
groups are less deactivating compared to crotonamide **55**. For the piperazine analogue **61**, it was theorized that it is sufficiently basic to deprotonate the sulfhydryl group of Cys442, thus rendering it more reactive. While potent in the enzyme assay, analogue **61**, however, did not show any potency in the cell-based assay.

Propargylamides **62** and **63** behaved similarly compared to the acrylamides in that the unsubstituted warhead was highly potent, while the methylated analogue was found to be inactive. Exploring cyanamide **64** as a structurally different class of electrophile led to a complete loss of activity.

The compounds in Table 4 were utilized to investigate whether the Itk activity of newly designed analogues could be predicted by computational methods. It was found that calculated electrophilicity, which is a measure of the reactivity of the different electrophiles, can be employed to generally predict the compounds' Itk inhibitory potency. The less reactive electrophiles, as calculated by lower electrophilicity values (e.g., <8 kcal/mol),³⁹ produce compounds devoid of activity against Itk ($IC_{50} > 100$ μ M). Conversely, attachment of a stronger electrophilic group to the pyrazolopyrimidine template yields analogues (such as **40** and **62**) with potent Itk inhibition ($IC_{50} = 10$ nM). While the variations for this set of analogues are focused on the reactive group that forms a covalent adduct with Cys442, the Itk activities overall appear to be primarily driven by the intrinsic chemical reactivity of the electrophile. The underlying assumption for this analysis is that the geometrical requirement for covalent bond formation is consistently met. The significance of this assumption is potentially reflected in the lack of activity of piperazine **60**, which based on its electrophilicity calculations should be the most potent Itk inhibitor in the present series.

In order to better understand the contribution of the electrophile to the potency of the covalent inhibitors and to expand the SAR information around the lipophilic back-pocket, additional acrylamides and their corresponding reversible acetamides were prepared. Table 5 highlights benzylamine- and aniline-based analogues.

Table 5. Demonstrating the Critical Nature of the Covalent Warhead for Itk Inhibition



Cpd#	R ₁	R ₂	ITK IC ₅₀ [μ M] (1 mM ATP)	ITK IC ₅₀ [μ M] (5 μ M ATP)
65	A	*-H	8.80	2.45
66	A	*-Me	>100	>100
67	B	*-H	1.68	0.07
68	B	*-Me	>100	>100
\pm -40	C	*-H	0.04	0.02
\pm -69	C	*-Me	>100	5.96
\pm -52	D	*-H	0.07	0.01
\pm -70	D	*-Me	>100	53.65
42	E	*-H	0.01	0.01
71	E	*-Me	>100	2.18
41	F	*-H	0.002	0.002

None of the reversible acetamides show potency in the presence of high ATP concentration, while only the acetamides incorporating *p*-isopropylphenyl (\pm -**69**) and *tert*-butylphenyl (\pm -**70** and **71**) show micromolar potency at low ATP concentrations. The incorporation of the electrophile leads to a substantial increase in potency independent from the ATP assay concentration.

An interesting observation can be made comparing covalent benzyl amides **65** and **42**. At physiological ATP concentrations, the presence of the lipophilic *p*-*tert*-butyl group leads to an increase in potency of essentially 3 orders of magnitude. Theoretical considerations suggest that this increase in potency cannot derive from merely a hydrophobic interaction but must involve a much stronger hydrogen bond network.⁴⁴ As was shown in Figure 4B, amide **52** engages Lys391 and Asp500 in two hydrogen bonds. Presumably, the sufficiently large lipophilic substituents at the terminal phenyl ring in **40**, **52**, **42**, and **41** act as anchors to position the aryl amide suitably to form the hydrogen bonds. The lack of this substituent (**65**) or a substituent of insufficient size (**67**) results in excessive flexibility of the distal phenyl ring and disruption of the hydrogen bonds with concomitant loss in potency.

The most potent amides **40**, **41**, \pm -**52**, and **42** were profiled in the cell-based IP1 assay as well as a whole-blood assay. In the IP1 assay, primary cells are treated with the inhibitor before anti-CD3 is added as a stimulus, and the inhibition of PLC γ phosphorylation, the immediate downstream target of Itk, is measured. Similarly, the whole-blood assay encompasses treatment with the inhibitor and stimulation with anti-CD3; however, the read-out is the detection of IL-2 production. As can be seen in Table 6,

Table 6. Cell Potencies and Kinetic Binding Data for Advanced Analogues

compd #	Itk IC ₅₀ [μ M] (5 μ M ATP, K_m)	IP1 IC ₅₀ [μ M]	hWB IC ₅₀ [μ M]	k_{inact}/K_i [1000/(M·s)]	$t_{1/2}$ [h]	Btk IC ₅₀ [μ M] (50 μ M ATP, K_m)
40	0.005	0.160	0.073	29.4	>24	0.005
41	0.002	0.031	0.048	16.1	>24	0.002
\pm -52	0.014	2.21	NA	NA	NA	0.015
42	0.005	0.516	6.731	18.6	>24	0.012
61	0.060	>50	NA	NA	NA	1.050

the potencies of compounds **40** and **41** translate well from the enzyme to cell and hWB assay, while amides \pm -**52**, **42**, and **61** show a significant loss in potency across the assays. The most potent compound **41** (PF-06465469)⁴³ in the enzyme assay is also the most potent compound in the IP1 and hWB assay.

A very interesting trend was observed among the compounds in Table 6 with respect to selectivity over Btk. Compounds **40** and **41** were virtually equipotent at both kinases in the presence of ATP concentrations corresponding to their respective K_m values. However, inhibitors **42** and **61** show selectivities, which trend toward the desired direction. The data implies that sufficient BTK selectivity could possibly be accomplished by suitable structural modifications at the distal phenyl ring as well as around the electrophilic warhead. The learnings from this SAR information are of significance for the future design of Itk inhibitors with improved selectivity.

In the context of covalent enzyme inactivation, time-dependent inhibition profiles of the inhibitors represent a critical means of characterization. Kinetic measurement of the binding event is an important technique of distinguishing covalent inhibitors.^{45,46} While amide **41** is the most potent inhibitor in the hWB assay,

its on-rate (k_{inact}/K_i) is about half compared to the second most potent analogue **40**. Analogue **42**, which shows only micromolar potency in the WB assay, is characterized by essentially the same on-rate as compound **41** (PF-06465469).⁴³ The three evaluated pyrazolopyrimidines display enzyme off-rates well beyond 24 h and thus can be characterized as truly irreversible inhibitors.

An analysis of IP1 cell potency vs enzyme potency determined in the presence of 1 mM ATP reveals that a correlation exists between the two assays (Figure 6). The moderate to low RRCK

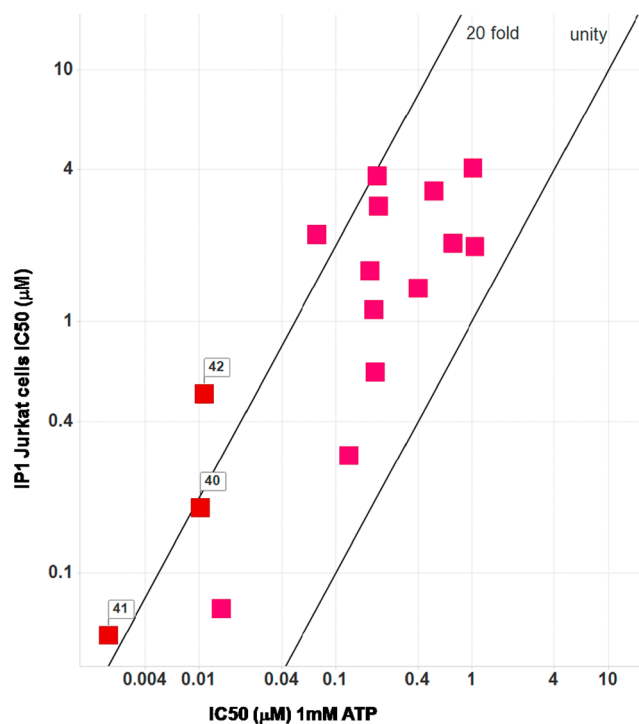


Figure 6. Reasonable correlation is observed (within approximately 20-fold) for potency data obtained from the cell-based IP1 and 1 mM ATP enzyme assay.

cell-permeability data for **40–42** shown in Table 7 may explain this series' left shift between the two assays.

Table 7 also highlights some calculated as well as physical and ADME properties of the most potent inhibitors reported in this series. The compounds reported here have reasonable topological polar surface area. The elevated clogP value is reflective of a moderate solubility and very high microsomal clearance, which leads to very short half-lives in the microsomal assay. The compounds in this series are moderately permeable and reasonably potent in the cell toxicity assay (THLE). The inhibitors are moderately potent in the dofetilide displacement assay, which gauges the compound's potency at the hERG ion channel. Together with the potencies reported in Table 6, compounds **40** and **41** (PF-06465469)⁴³ show a promising level of ligand efficiency (LE) and lipophilic ligand efficiency (LipE).

To better depict the overall progress of the covalent Itk inhibitors with respect to LipE, a correlation of pIC_{50} and clogP was plotted with LipE lines entered as shown in Figure 7.

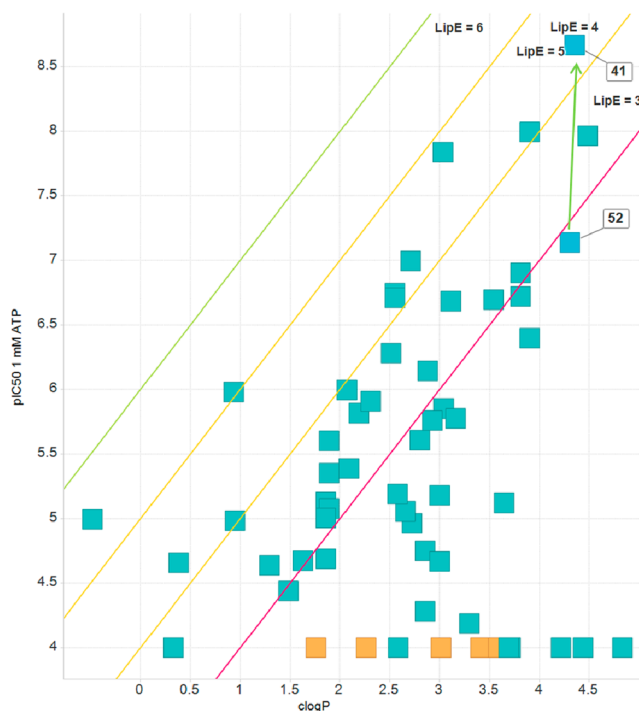


Figure 7. A pIC_{50} vs clogP plot reveals that among the acrylamides (cyan) several of them are potent and show LipE values in the 4–5 range; the noncovalent acetamides (Table 5) are included as well (orange).

While a large portion of the compounds are in a very low LipE space (≤ 3), a good number of potent inhibitors show a LipE in the 4–5 range. However, in order to reach an acceptable LipE ≥ 6 , a significant reduction of the series' clogP range would have to be accomplished without compromising enzyme and whole-blood potency. A reduction of clogP would most likely also lead to an improvement of the series' HLM clearance properties.

In conclusion, we have discovered novel and potent covalent inhibitors of Itk. The extremely low K_m of ATP for Itk (5 μM) represents a significant hurdle for inhibiting Itk in a cellular environment. To drive this program effectively, the present covalent compounds were all assessed in the presence of a physiologically relevant ATP concentration (1 mM). The disclosed electrophilic acrylamides display a wide range of potencies under the assay conditions. However, the corresponding acetamide analogues of several of the most potent acrylamides are essentially inactive in the presence of 1 mM ATP suggesting that the electrophilic nature of the compounds plays a dominant role in the inhibition event.

Crucial to the covalent inhibition strategy of this project is the half-life at which Itk is regenerated within cells. A traditional pulse–chase experiment yielded a value of about 2 h. A more informative experiment in which inhibition of the generation of

Table 7. Calculated, Physical, and ADMET Properties for Advanced Analogues

compd #	TPSA	clogP	sol. [μM] pH 6.5	CLint HLM [$\mu\text{L}/(\text{min}\cdot\text{mg})$]	$t_{1/2}$ HLM [min]	RRCK AB [$10^{-6}\text{cm}^2\cdot\text{s}^{-1}$]	THLE IC_{50} [μM]	DOF IC_{50} [μM]	LE	LipE
40	119	3.9	7.6	>320	<3	1.4	5.9	1.1	0.29	4.09
41	119	4.4	10.6	200	5	<0.1	8.0	0.3	0.31	4.31
42	119	4.5	6.0	>227	<5	8.5	32.3	1.8	0.27	3.48

phospho-PLC γ 1 was measured following covalent Itk inhibition, however, showed that the inhibitory effect can last for up to 24 h. This finding was critical to validating the strategy of a covalent inhibition approach to Itk.

Structural information was utilized to guide the design of a library in which the distal phenyl ring of the biaryl amide motif was varied to optimize physical properties without compromising potency. This effort has provided potent covalent analogues featuring a biaryl amide bond crucial for Itk potency. The SAR information, however, strongly suggests a highly lipophilic pocket into which this aromatic group binds. The acrylamide analogue **41** (PF-06465469)⁴³ with the 3-methyl-4-isopropylphenyl benzamide substituent was the most potent inhibitor in the enzyme assay in the presence of 1 mM ATP. When tested in the IP1 and hWB cell-based assays, this compound was found to be highly potent with IC₅₀s of 31 and 48 nM, respectively. Kinetic measurements to determine the inhibitor's enzyme on- and off-rates yielded results that indicated that the acrylamide has a decent on-rate and is irreversibly bound to the enzyme. X-ray crystal structures of related analogues feature the covalent interaction of the acrylamide with Cys442. The crystallographic analysis further revealed significant ligand–protein hydrogen bond interactions of the acrylamide carbonyl and the pyrazolopyrimidine scaffold as well as the N–H and carbonyl of the diarylamide. Itk's high sequence homology with Btk (70% for the binding site) as well as the reduced nucleophilicity of Cys442 resulting from its elevated pK_a have defined selectivity as a major parameter for the advancement of the current series. However, the SAR information obtained from the presented analogues together with crystal structure information will prove to be critical to devise strategies for improving this series' selectivity profile as well as physical properties.

■ GENERAL SYNTHETIC PROCEDURES

Chemistry Methods and Compound Characterization. Proton (¹H NMR) and carbon (¹³C NMR) magnetic resonance spectra were obtained in DMSO-*d*₆ at 400 and 100 MHz, respectively, unless otherwise noted. The following abbreviations were utilized to describe peak patterns when appropriate: br = broad, s = singlet, d = doublet, and m = multiplet. High-resolution mass measurements were obtained on an Agilent ToF mass spectrometer. Accurate Mass Spectrometry analyses were conducted on an Agilent 6220 TOF mass spectrometer (Agilent Technologies, Wilmington, DE) in positive or negative electrospray mode. The system was calibrated to greater than 1 ppm accuracy across the mass range prior to analyses according to manufacturer's specifications. The samples were separated using UHPLC on an Agilent 1200 (Agilent Technologies, Wilmington, DE) system prior to mass spectrometric analysis. The resulting spectra were automatically lockmass corrected, and the target mass ions and any confirming adducts (Na⁺, NH₄⁺) were extracted and combined as a chromatogram. The mass accuracy was calculated for all observed isotopes against the theoretical mass ions derived from the chemical formula using MassHunter software (Agilent Technologies, Wilmington, DE). All air and moisture sensitive reactions were carried out under an atmosphere of dry nitrogen using heat-dried glassware and standard syringe techniques. Tetrahydrofuran (THF) and acetonitrile were purchased from EMD anhydrous and were used without further drying. All final compounds were isolated following flash chromatography, which was performed using an Analogix Intelliflash 280 with Septra Si 50 silica gel utilizing ethyl acetate/heptane mixtures as solvent unless otherwise indicated. All compounds submitted for biological testing and reported in this article were obtained in ≥95% purity unless otherwise noted. Certain compounds from the examples described were purified on reversed-phase using automated preparative high performance liquid chromatography (HPLC) on a Gilson GX281, Shimadzu CL-2010C, or Agilent 1200 system. Samples were submitted dissolved

in 1 mL of DMSO. Depending on the nature of the compounds and the results of a preanalysis, the purification was performed under a variety of conditions at ambient temperature. HPLC was carried out on an Agella Venusil ASB C18 column (21.2 × 150 mm, 5 μm). A flow rate of 0.5–150 mL/min was used with mobile phase A, water + 0.1% modifier (v/v), and B, acetonitrile + 0.1% modifier (v/v). The modifier was formic acid, trifluoroacetate, ammonia acetate, or hydrochloric acid. A Shimadzu MS2010EV MS2525 binary LC or Waters 2545 BGM pump supplied a mobile phase with a composition of 5% B for 1 min then ran from 5% to 98% B over 6 min followed by a 2 min hold at 98% B. Detection was achieved using a Shimadzu SPD-20AV or Waters 2998 PDA wavelength absorbance detector set at 220 or 200 nm followed in series by a Shimadzu MS2010EV or Waters 3100 mass spectrometer.

Quality control (QC) analysis was performed using a LC-MS method. Acidic runs were carried out on a Shimadzu XB-C18 (2.1 × 30 mm, 5 μm), X-Bridge (50 × 4.6 mm, 5 μm), Gemini NX C18 (50 × 4.6, 3 μm), or Gemini NX C18 (50 × 4.6, 5 μm). A flow rate of 1.0–1.2 mL/min was used with mobile phase A, water + 0.1% modifier (v/v), and B, acetonitrile + 0.1% modifier (v/v). For acidic runs, the modifier was trifluoroacetic acid. A Shimadzu 20AB pump ran a gradient elution from 0% to 98% B over 2 min followed by a 1 min hold at 95% B. Detection was achieved using a Shimadzu 10A detector set at 220 or 260 nm followed in series by a Shimadzu MS2010EV or Applied Biosystem API 2000 mass spectrometer in parallel.

(R)-tert-Butyl 3-(4-Amino-3-iodo-1H-pyrazolo[3,4-d]pyrimidin-1-yl)piperidine-1-carboxylate (8). To a mixture of 3-Iodo-1H-pyrazolo[3,4-d]pyrimidin-4-amine **6** (1.27 g, 4.87 mmol, 1.0 equiv) in THF (150 mL) was added triphenyl phosphine (1.95 g, 7.30 mmol, 1.5 equiv), diisopropylidene-1,2-dicarboxylate (1.54 mL, 7.30 mmol, 1.5 equiv), and (S)-tert-butyl 3-hydroxypiperidine-1-carboxylate **7** (1.96 g, 9.73 mmol, 2.0 equiv) at room temperature. The reaction was stirred for 16 h and was judged complete by LC-MS. The reaction was concentrated to a residue and purified via column chromatography (0% ethyl acetate in dichloromethane to 80%) to provide the desired material as a white solid (1.33 g, 83%). ¹H NMR (400 MHz, CDCl₃) δ = 1.45 (s, 9 H), 1.55–1.77 (m, 1 H), 1.80–1.96 (m, 1 H), 2.08–2.29 (m, 1 H), 2.74–2.94 (m, 1 H), 3.6–3.49 (m, 1 H), 4.12 (q, J = 7.0 Hz, 2 H), 4.64–4.86 (m, 1 H), 6.45 (br. s., 2 H), 8.31 (s, 1 H). LC-MS: 98%, m/z = 445.1 [M + H]; Chiral HPLC (ChiralPak AS-H, 4.6 × 100 mm, 5 μm, heptane/ethanol) = 98% e.e.

(R)-1-(3-(4-Amino-3-(4-methoxyphenyl)-1H-pyrazolo[3,4-d]pyrimidin-1-yl)piperidin-1-yl)prop-2-en-1-one (10). **Step 1:** In a sealed tube containing **8** (1.0 g, 2.255 mmol, 1.0 equiv), 4-methoxyphenyl boronic acid (0.48 g, 3.158 mmol, 1.4 equiv) and potassium carbonate (0.62 g, 4.511 mmol, 2.0 equiv) in 1,4-dioxane (50 mL) was purged under argon for 15 min. PdCl₂(dppf)₂ (92 mg, 0.112 mmol, 0.05 equiv) was added and again purged under argon for 10 min. The reaction mixture was heated to 120 °C for 12 h. TLC showed the completion of the reaction. The reaction mixture was filtered through a Celite bed, and the filtrate was concentrated and purified by column chromatography (60% ethyl acetate in petroleum ether) to provide **9a** as a white solid (0.60 g, 62%). ¹H NMR (300 MHz, DMSO-*d*₆): δ = 1.4 (s, 9H), 1.6 (m, 2H), 2.1 (m, 2H), 3.0 (m, 2H), 3.9 (s, 3H), 4.0 (m, 2H), 4.7 (m, 1H), 6.8 (bs, 2H), 7.1 (d, 2H), 7.6 (d, 2H), 8.2 (s, 1H). LC-MS: 76.4%, m/z = 425.0 [M + H].

To stirred solution of **9a** (0.7 g, 1.65 mmol, 1.0 equiv) in 1,4 dioxane (10 mL) at 0 °C was added 4 N HCl in dioxane (15 mL). The reaction mixture was stirred at room temperature for 4 h. After complete conversion of the starting material, excess 1,4-dioxane was removed under vacuum and to the residue was added ethyl acetate and water. The water layer was basified with 2 N NaHCO₃ solution and extracted with ethyl acetate. The organic layer was then washed with water followed by brine. The organic layer was dried over sodium sulfate, filtered, and concentrated to provided the deprotected piperidine (0.45 g, 84%). ¹H NMR (300 MHz, DMSO): δ = 1.6 (m, 2H), 1.8 (m, 2H), 2.1 (m, 2H), 3.0 (m, 2H), 3.1 (d, 1H), 3.9 (s, 3H), 4.7 (m, 1H), 7.1 (d, 2H), 7.6 (m, 4H), 8.2 (s, 1H). LC-MS: 83.4%; m/z = 325.1 [M + H].

Step 2: To a stirred solution of acrylic acid (0.095 mL, 1.388 mmol, 1.0 equiv), EDCI (0.399 g, 2.0832 mmol, 1.5 equiv), HOBT (0.318 g, 2.0832 mmol, 1.5 equiv), and triethylamine (0.39 mL, 2.776 mmol, 2.0 equiv) in

THF (40 mL) at 0 °C was added the deprotected piperidine (0.45 g, 1.388 mmol, 1.0 equiv). Reaction mixture was stirred at room temperature for 24 h. After complete consumption of the starting material, the reaction was diluted with ethyl acetate and water. The organic layer was dried over sodium sulfate and evaporated to get crude **10** (0.5 g crude). The crude compound was purified by prep TLC to provide **10**. ¹H NMR (300 MHz, DMSO): δ = 1.6 (m, 2H), 1.9 (m, 1H), 2.1 (m, 1H), 3.1 (m, 2H), 3.9 (s, 3H), 4.2 (m, 2H), 4.6 (m, 1H), 4.7 (m, 1H), 5.7 (dd, 1H), 6.1 (t, 1H), 6.7 to 6.9 (m, 2H), 7.1 (d, 2H), 7.6 (d, 2H), 8.2 (s, 1H). LC-MS: 88.8%, *m/z* = 378.9 [M + H]; HRMS [M + H] for C₂₀H₂₃N₆O₂, calcd, 379.1877; found, 379.1880.

(R)-1-(3-(4-Amino-3-(3-methoxyphenyl)-1H-pyrazolo[3,4-d]pyrimidin-1-yl)piperidin-1-yl)prop-2-en-1-one (11). **Step 1:** By following a procedure similar to that for **9a**, **8** (1.0 g, 2.255 mmol, 1.0 equiv) was converted into **9b** (0.6 g, 62%). ¹H NMR (300 MHz, DMSO-*d*₆): δ = 1.4 (s, 9H), 1.6 (m, 2H), 2.1 (m, 2H), 3.0 (m, 2H), 3.9 (s, 3H), 4.0 (m, 2H), 4.7 (m, 1H), 7.0 (d, 1H), 7.15 (s, 1H), 7.2 (d, 1H), 7.5 (t, 1H), 7.6 (bs, 2H), 8.3 (s, 1H). LC-MS: 74.4%, *m/z* = 425.0 [M + H].

Step 2: Compound **9b** (0.7 g, 1.6509 mmol, 1.0 equiv) was deprotected by following a procedure similar to that for the deprotection of **9a**, providing the free piperidine (0.45 g, 84%). ¹H NMR (300 MHz, DMSO): δ = 1.6 (m, 2H), 1.8 (m, 2H), 2.1 (m, 2H), 3.0 (m, 2H), 3.1 (d, 1H), 3.9 (s, 3H), 4.7 (m, 1H), 7.1 (d, 1H), 7.2 (s, 1H), 7.25 (d, 1H), 7.4 to 7.6 (m, 3H), 8.3 (s, 1H). LC-MS: 86.2%, *m/z* = 325.1 [M + H].

Step 3: By following a procedure similar to that for target **10**, the deprotected piperidine (0.12 g, 0.3703 mmol, 1.0 equiv) was converted into **11** (15 mg, 10%). LC-MS (95.74%, M + H). ¹H NMR (300 MHz, DMSO): δ = 1.6 (m, 1H), 1.9 (m, 1H), 2.1 (m, 1H), 2.3 (m, 1H), 3.0 (m, 1H), 3.2 (m, 1H), 3.9 (s, 3H), 4.1 (m, 1H), 4.2 (m, 1H), 4.5 (m, 1H), 4.7 (m, 1H), 5.6 to 5.7 (m, 1H), 6.1 (m, 1H), 6.7 to 6.9 (m, 2H), 7.1 (d, 1H), 7.2 (s, 1H), 7.25 (d, 1H), 7.5 (t, 1H), 8.3 (s, 1H); HRMS [M + H] for C₂₀H₂₃N₆O₂, calcd, 379.1877; found, 379.1881.

Suzuki Library. Step 1: To a solution of template (125 μmol, 1.0 equiv) in anhydrous 1,4-dioxane (625 μL) was added a solution of boronic acid monomer (125 μmol, 1.0 equiv) in anhydrous 1,4-dioxane (625 μL). The solution was degassed thoroughly. To the solution was added PdCl₂(dppf) (6 mg, 7.5 μmol, 0.6 equiv) followed by anhydrous K₂CO₃ (52 mg, 375 μmol, 3 equiv). The reaction was stirred under argon at 90 °C for 16 h and monitored by LC-MS. The reaction mixture was filtered through a Celite bed and washed with 1,4-dioxane, and solvent was evaporated in a thermo explorer (2 h, 5 Torr, and 45 °C). The residue was dissolved in ethyl acetate (5 mL) and washed with water (1 × 3 mL) and brine (1 × 3 mL). The organic layer was dried over anhydrous sodium sulfate and evaporated under reduced pressure.

Step 2: The residue from the previous step was dissolved in 1,4-dioxane (500 μL), transferred to reaction vials, and cooled to 0 °C. To the reaction was added 1,4-dioxane-HCl (500 μL), and the reaction was stirred for 16 h at 25 °C. The solvent was evaporated under reduced pressure and azeotroped with toluene to provide a residue that was used in step 3 without further purification.

Step 3: To a solution of acrylic acid (250 mg, 3.5 mmol) in DCM (20 mL) was added thionyl chloride (5.2 mmol, 0.38 mL, 1.5 equiv). The reaction was heated at 40 °C for 4 h. Half of the total volume of DCM was evaporated. The residue from the previous step was dissolved in DCM (1 mL), and TEA (70 μL, 5.0 equiv) was added to the reaction vial. To the reaction was added acryloyl chloride solution (300 μL) at 0 °C. Reaction vials were stirred at 0 °C for 10–15 min after which it was quenched with ice, and the solvent was evaporated. All the compounds were dissolved in 100% DMSO. Ten microliters from each well was transferred to a daughter plate and diluted with 200 μL of DMSO. LC-MS of crude compounds were done, and these were further purified on Waters Autopurification System (Column: Luna Phenyl Hexyl (21 × 150 mm, 10 μm), with mobile phase A, 10 mM ammonium acetate in water, and B, acetonitrile. *T* = 0; flow = 20; A = 90%; B = 10%; *T* = 3; flow = 20; A = 75%; B = 25%; *T* = 18;

flow = 20; A = 35%; B = 65%.) Prep fractions were collected in bar coded test tubes and evaporated in a Thermo explorer (40 °C, 15 Torr, 16 h). Each of the compounds were then dissolved in ethanol (1.6 mL) and transferred to pretared 2 drum glass vials. Finally they were dried in Genevac first for 1 h (at 40 °C, 10 mbar) and then for 12 h (at 40 °C, 0 mbar). Weights were taken using Mettler Balance. These compounds were then dissolved in a calculated amount of DMSO to prepare a 30 mM solution. Eight microliters was removed for final QC analysis (diluted with 150 μL of DMSO) on an analytical LC/MS. QC reports were generated to check the identity and purity of each compound.

12: LC-MS 100%, min 1.67, *m/z* = 417.18 [M + H]; HRMS [M + H] for C₂₀H₂₀F₃N₆O, calcd, 417.1645; found, 417.1650.

13: LC-MS 88.4%, min 1.69, *m/z* = 417.21 [M + H]; HRMS [M + H] for C₂₀H₂₀F₃N₆O, calcd, 417.1645; found, 417.1650.

14: LC-MS 95.10%, min 1.68, *m/z* = 433.16 [M + H]; HRMS [M + H] for C₂₀H₂₀F₃N₆O₂, calcd, 433.1594; found, 433.1599.

15: LC-MS 100%, min 1.72, *m/z* = 433.21 [M + H].

16: LC-MS 96.1%, min 1.49, *m/z* = 409.28 [M + H]; HRMS [M + H] for C₂₁H₂₅N₆O₃, calcd, 409.1983; found, 409.1987.

17: LC-MS 95.8%, min 1.53, *m/z* = 407.21 [M + H]; HRMS [M + H] for C₂₁H₂₃N₆O₃, calcd, 407.1826; found, 407.1829.

18: LC-MS 100%, min 1.38, *m/z* = 379.35 [M + H]; HRMS [M + H] for C₂₀H₂₃N₆O₂, calcd, 379.1877; found, 379.1883.

19: LC-MS 100%, min 1.50, *m/z* = 380.23 [M + H]; HRMS [M + H] for C₁₉H₂₂N₇O₂, calcd, 380.1829; found, 380.1835.

29: LC-MS 100%, 1.24 min, *m/z* = 379.19 [M + H]; HRMS [M + H] for C₁₉H₂₃N₈O, calcd, 379.1989; found, 379.1990.

21: LC-MS 100%, 1.37 min, *m/z* = 351.21 [M + H]; HRMS [M + H] for C₁₇H₁₉N₈O, calcd, 351.1676; found, 351.1675.

22: LC-MS 81.4%, min 1.58, *m/z* = 400.23 [M + H]; HRMS [M + H] for C₂₂H₂₂N₇O, calcd, 400.1880; found, 400.1886.

23: LC-MS 100%, min 1.46, *m/z* = 400.19 [M + H]; HRMS [M + H] for C₂₂H₂₂N₇O, calcd, 400.1880; found, 400.1885.

24: LC-MS 100%, min 1.50, *m/z* = 400.28 [M + H]; HRMS [M + H] for C₂₂H₂₂N₇O, calcd, 400.1880; found, 400.1884.

25: LC-MS 100%, min 1.41, *m/z* = 411.21 [M + H].

26: LC-MS 100%, min 1.44, *m/z* = 425.25 [M + H].

27: LC-MS 100%, min 1.43, *m/z* = 427.23 [M + H]; HRMS [M + H] for C₂₀H₂₃N₆O₃S, calcd, 427.1547; found, 427.1551.

(R)-3-(1-(1-Acryloylpiperidin-3-yl)-4-amino-1H-pyrazolo[3,4-d]pyrimidin-1-yl)-N-(4-isopropylphenyl)benzamide (40). **Step 1:** Diimidazol-1-yl-methanone (649 mg, 4 mmol) was added to the suspension of 3-[4-amino-3-(3-carboxyphenyl)pyrazolo[3,4-d]pyrimidin-1-yl]-piperidine-1-carboxylic acid *tert*-butyl ester (877 mg, 2 mmol) in dichloromethane (8 mL), and the mixture was stirred for 30 min. Then 4-isopropylphenylamine (595 mg, 4.4 mmol) was added, and the mixture was stirred for 30 min. The solvent was removed under reduced pressure, and the mixture was purified by column chromatography (2% methanol in dichloromethane) to afford 3-[4-amino-3-[3-(4-isopropylphenylcarbamoyl)phenyl]pyrazolo[3,4-d]pyrimidin-1-yl]-piperidine-1-carboxylic acid *tert*-butyl ester (840 mg, 76%) as a white solid.

Step 2: To a solution of 3-[4-amino-3-[3-(4-isopropylphenylcarbamoyl)phenyl]pyrazolo[3,4-d]pyrimidin-1-yl]piperidine-1-carboxylic acid *tert*-butyl ester (778 mg, 1.4 mmol, 1.0 equiv) in dioxane (4.2 mL) was added 4 N HCl in dioxane (2.1 mL, 8.4 mmol, 6.0 equiv). The reaction mixture was refluxed for 30 min, and the solvent was removed under reduced pressure to afford 3-[4-amino-3-[3-(4-isopropylphenylcarbamoyl)phenyl]pyrazolo[3,4-d]pyrimidin-1-yl]piperidinium chloride (689 mg, 100%) as an off-white solid.

Step 3: Triethylamine (152 mg, 1.5 mmol) followed by acryloyl chloride (50 mg, 550 μmol) was added to the suspension of 3-[4-amino-3-[3-(4-isopropylphenylcarbamoyl)phenyl]pyrazolo[3,4-d]pyrimidin-1-yl]piperidinium chloride (246 mg, 500 μmol) in dichloromethane (1.5 mL) at 0 °C while stirring. The cooling bath was removed, and the mixture was stirred for 30 min. The mixture was then directly purified by column chromatography (0% methanol in dichloromethane to 7%) to afford **40** (136 mg, 53%) as a colorless glass. ¹H NMR (400 MHz, DMSO-*d*₆): δ = 1.22 (d, *J* = 6.63 Hz, 6 H), 1.54–1.70 (m, 2 H),

1.90–2.40 (m, 3 H), 2.82–2.94 (m, 1 H), 3.01–3.75 (m, 2 H), 4.01–4.30 (m, 1 H), 4.54–4.87 (m, 1 H), 5.56–6.40 (m, 1 H), 6.68–6.95 (m, 1 H), 7.25 (d, $J = 8.59$ Hz, 2 H), 7.63–7.77 (m, 3 H), 7.88 (d, $J = 7.41$ Hz, 1 H), 8.07 (d, $J = 7.81$ Hz, 1 H), 8.25 (br. s., 1 H), 8.30 (s, 1 H) 10.29 (br. s., 1 H); LC-MS: 99%, $m/z = 510.3$ [M + H].

Chiralcel OJ-H RT = 5.20 min. ^1H NMR (400 MHz, DMSO- d_6): $\delta = 1.22$ (d, $J = 6.63$ Hz, 6 H), 1.54–1.70 (m, 2 H), 1.90–2.40 (m, 3 H), 2.82–2.94 (m, 1 H), 3.01–3.75 (m, 2 H), 4.01–4.30 (m, 1 H), 4.54–4.87 (m, 1 H), 5.56–6.40 (m, 1 H), 6.68–6.95 (m, 1 H), 7.25 (d, $J = 8.59$ Hz, 2 H), 7.63–7.77 (m, 3 H), 7.88 (d, $J = 7.41$ Hz, 1 H), 8.07 (d, $J = 7.81$ Hz, 1 H), 8.25 (br. s., 1 H), 8.30 (s, 1 H) 10.29 (br. s., 1 H). LC-MS: 100%, $m/z = 510.0$ [M + H]; HRMS [M + H] for $\text{C}_{29}\text{H}_{32}\text{N}_7\text{O}_2$, calcd, 510.2612; found, 510.2614.

(*R*)-3-(1-(1-Acryloylpiperidin-3-yl)-4-amino-1H-pyrazolo[3,4-*d*]-pyrimidin-3-yl)-*N*-(4-*tert*-butylbenzyl)benzamide (42). **Step 1:** To a stirred solution of compound 28 (150 mg, 0.342 mmol) in DMF (3 mL) was added DIPEA (132.4 mg, 1.03 mmol), HATU (143 mg, 0.376 mmol), and (4-*tert*-butyl) benzylamine (56 mg, 0.342 mmol) at 0 °C. The reaction mixture was stirred at room temperature for 16 h. It was quenched with ice water and extracted with ethyl acetate (3 × 50 mL). The organic layer was washed with water (2 × 20 mL) followed by brine (1 × 20 mL), dried over sodium sulfate, and was evaporated to dryness. The crude mass was purified by column chromatography (20% ethyl acetate in hexane) to afford compound 29c (140 mg, 70%) as a brown solid. ^1H NMR (400 MHz, DMSO- d_6): $\delta = 1.26$ (s, 9 H), 1.34 (s, 9 H), 2.65–2.46 (m, 1 H), 1.91 (br s, 1 H), 2.10–2.06 (m, 1 H), 2.28–2.24 (m, 1 H), 3.04 (br s, 1 H), 3.91 (br s, 1 H), 4.46 (d, 2 H), 4.69 (br s, 1 H), 7.25 (d, 2 H), 7.34 (d, 2 H), 7.63 (t, 1 H), 7.79 (d, 1 H), 7.98 (d, 1 H), 8.18 (s, 1 H), 8.27 (s, 1 H), 9.10–9.09 (m, 1 H); LC-MS: $m/z = 584.2$ [M + H].

Step 2: To a stirred solution of compound 29c (140 mg, 0.216 mmol) in dioxane (1 mL) was added 4 N HCl in dioxane (7 mL) at 0 °C, and it was stirred at room temperature for 3 h. Then excess dioxane was evaporated. The reaction residue was triturated with *n*-pentane. The solid was collected by filtration and was dried to afford the deprotected piperidine. This off-white solid (115 mg, 86%) was directly used for the next step as the HCl salt. LC-MS: $m/z = 484.6$ [M + H].

Step 3: To a stirred solution of the deprotected piperidine (115 mg, 0.207 mmol) in DMF (2 mL) was added the BOP reagent (91.5 mg, 0.207 mmol) followed by DIPEA (0.089 mL, 0.518 mmol) and acrylic acid (15 mg, 0.189 mmol). The reaction mixture was stirred at room temperature for 15 min. It was quenched with ice water and filtered. The residue was dissolved in ethyl acetate, dried over sodium sulfate, and was concentrated to dryness. The crude material was purified by prep-HPLC to afford the desired material 42 as a white solid (43 mg, 39%). ^1H NMR (400 MHz, DMSO- d_6 , 100 °C): $\delta = 1.30$ (s, 9H), 1.68–1.62 (m, 1H), 1.99–1.96 (m, 1H), 2.30 (m, 1H), 2.36 (m, 1H), 3.20–3.14 (m, 1H), 3.55 (m, 1H), 4.12–4.08 (m, 1H), 4.42–4.39 (m, 1H), 4.50 (d, 2H), 4.79–4.74 (m, 1H), 5.66–5.60 (m, 1H), 6.07–6.03 (m, 1H), 6.07–6.03 (m, 1H), 6.53 (s, 2H), 6.74–6.67 (m, 1H), 7.37–7.28 (m, 4H), 7.63 (t, 1H), 7.81 (d, 1H), 7.99 (d, 1H), 8.18 (s, 1H), 8.28 (s, 1H), 8.74 (s, 1H). HPLC purity: 96.12%; HRMS [M + H] for $\text{C}_{30}\text{H}_{34}\text{N}_7\text{O}_2$, calcd, 524.2768; found, 524.2769.

3-(1-(1-Acryloylpiperidin-3-yl)-4-amino-1H-pyrazolo[3,4-*d*]-pyrimidin-3-yl)-*N*-cyclohexylbenzamide (49). **Step 1:** Diimidazol-1-yl-methanone (649 mg, 4 mmol, 2.0 equiv) was added to the suspension of 3-[4-amino-3-(3-carboxyphenyl)pyrazolo[3,4-*d*]pyrimidin-1-yl]-piperidine-1-carboxylic acid *tert*-butyl ester (877 mg, 2 mmol, 1.0 equiv) in dichloromethane (8 mL), and the mixture was stirred for 30 min. Subsequently, cyclohexylamine (436 mg, 4.4 mmol, 2.2 equiv) was added, and the mixture was stirred for 30 min. Then, the solvent was removed under reduced pressure, and the residue was separated by column chromatography (2% methanol in dichloromethane) to afford 3-{4-amino-3-[3-(cyclohexylcarbamoyl)phenyl]pyrazolo[3,4-*d*]pyrimidin-1-yl}piperidine-1-carboxylic acid *tert*-butyl ester (921 mg, 89%) as a white solid.

Step 2: To a solution of 3-{4-amino-3-[3-(3-*tert*-butylphenylcarbamoyl)phenyl]pyrazolo[3,4-*d*]pyrimidin-1-yl}piperidine-1-carboxylic acid *tert*-butyl ester (912 mg, 1.6 mmol, 1.0 equiv) in dioxane (4.8 mL) was added 4 N HCl in dioxane (2.4 mL, 9.6 mmol, 6.0 equiv). The reaction

mixture was refluxed for 30 min, and the solvent was removed under reduced pressure to afford 3-{4-amino-3-[3-(3-*tert*-butylphenylcarbamoyl)phenyl]pyrazolo[3,4-*d*]pyrimidin-1-yl}piperidinium chloride (729 mg, 100%) as a white solid.

Step 3: Triethylamine (152 mg, 1.5 mmol) followed by acetyl chloride (43 mg, 550 μmol) was added to the suspension of 3-{4-amino-3-[3-(3-*tert*-butylphenylcarbamoyl)phenyl]pyrazolo[3,4-*d*]pyrimidin-1-yl}piperidinium chloride (228 mg, 500 μmol) in dichloromethane (1.5 mL) at 0 °C while stirring. The cooling bath was removed, and the mixture was stirred for 30 min. The mixture was then directly purified by column chromatography (0% methanol in dichloromethane to 7%) to afford compound 49 (100 mg, 42%) as a colorless glass. ^1H NMR (400 MHz, DMSO- d_6): $\delta = 1.04$ –1.41 (m, 4 H), 1.46–2.38 (m, 8 H), 2.93–3.27 (m, 1 H), 3.11–3.26 (m, 1 H), 3.64–3.89 (m, 2 H), 3.99–4.28 (m, 2 H), 4.50–4.81 (m, 2 H), 5.56–5.74 (m, 1 H), 6.05–6.20 (m, 1 H), 6.65–6.94 (m, 1 H), 7.61 (d, $J = 8.05$ Hz, 1 H), 7.76 (br. s., 1 H), 7.93 (d, $J = 8.05$ Hz, 1 H), 8.10 (br. s., 1 H), 8.26 (br. s., 1 H), 8.31 (d, $J = 8.05$ Hz, 1 H). LC-MS: 100%, $m/z = 474.3$ [M + H]; HRMS [M + H] for $\text{C}_{26}\text{H}_{32}\text{N}_7\text{O}_2$, calcd, 474.2612; found, 474.2615.

3-(1-(1-Acryloylpiperidin-3-yl)-4-amino-1H-pyrazolo[3,4-*d*]pyrimidin-3-yl)-*N*-(3-*tert*-butylphenyl)benzamide (52). **Step 1:** Diimidazol-1-yl-methanone (649 mg, 4 mmol) was added to the suspension of 3-[4-amino-3-(3-carboxyphenyl)pyrazolo[3,4-*d*]pyrimidin-1-yl]-piperidine-1-carboxylic acid *tert*-butyl ester (877 mg, 2 mmol) in dichloromethane (8 mL), and the mixture was stirred for 30 min. Then, 3-*tert*-butylphenylamine (657 mg, 4.4 mmol) was added, and the mixture was stirred for 30 min. Then, the solvent was removed under reduced pressure, and the residue was separated by column chromatography (2% methanol in dichloromethane) to afford 3-{4-amino-3-[3-(3-*tert*-butylphenylcarbamoyl)phenyl]pyrazolo[3,4-*d*]pyrimidin-1-yl}piperidine-1-carboxylic acid *tert*-butyl ester (1.09 g, 96%) as a white solid.

Step 2: To a solution of 3-{4-amino-3-[3-(3-*tert*-butylphenylcarbamoyl)phenyl]pyrazolo[3,4-*d*]pyrimidin-1-yl}piperidine-1-carboxylic acid *tert*-butyl ester (912 mg, 1.6 mmol, 1.0 equiv) in dioxane (4.8 mL) was added 4 N HCl in dioxane (2.4 mL, 9.6 mmol, 6.0 equiv). The reaction mixture was refluxed for 30 min, and the solvent was removed under reduced pressure to afford 3-{4-amino-3-[3-(3-*tert*-butylphenylcarbamoyl)phenyl]pyrazolo[3,4-*d*]pyrimidin-1-yl}piperidinium chloride (810 mg, 100%) as a colorless glass.

Step 3: Triethylamine (152 mg, 1.5 mmol) followed by acryloyl chloride (50 mg, 550 μmol , 1.1 equiv) was added to the suspension of 3-{4-amino-3-[3-(3-*tert*-butylphenylcarbamoyl)phenyl]pyrazolo[3,4-*d*]pyrimidin-1-yl}piperidinium chloride (253 mg, 500 μmol , 1.0 equiv) in dichloromethane (1.5 mL) at 0 °C while stirring. The cooling bath was removed, and the mixture was stirred for 30 min. The mixture was then directly purified by column chromatography (0% methanol in dichloromethane to 7%) to afford 52 (187 mg, 71%) as a colorless glass. ^1H NMR (400 MHz, DMSO- d_6): $\delta = 1.13$ –1.42 (m, 9 H), 1.49–1.72 (m, 1 H), 1.80–2.41 (m, 3 H), 3.00–3.77 (m, 2 H), 3.95–4.29 (m, 1 H), 4.53–4.84 (m, 1 H), 5.47–6.34 (m, 1 H), 5.94–6.27 (m, 1 H), 6.60–6.95 (m, 1 H), 7.15 (d, $J = 8.05$ Hz, 2 H), 7.28 (t, $J = 8.05$ Hz, 1 H), 7.65–7.74 (m, 2 H), 7.80 (br. s., 1 H), 7.87 (d, $J = 6.59$ Hz, 1 H), 8.06 (d, $J = 8.05$ Hz, 1 H), 8.23–8.30 (m, 2 H), 10.28 (s, 1 H); HPLC = 100%; HRMS [M + H] for $\text{C}_{30}\text{H}_{32}\text{N}_7\text{O}_2$, calcd, 524.2774; found, 524.2891.

(*S*)-3-(1-(1-Acryloylpiperidin-3-yl)-4-amino-1H-pyrazolo[3,4-*d*]pyrimidin-3-yl)-*N*-(4-isopropylphenyl)benzamide (53). Chiralcel OJ-H RT = 4.49 min. ^1H NMR (400 MHz, DMSO- d_6): $\delta = 1.22$ (d, $J = 6.63$ Hz, 6 H), 1.54–1.70 (m, 2 H), 1.90–2.40 (m, 3 H), 2.82–2.94 (m, 1 H), 3.01–3.75 (m, 2 H), 4.01–4.30 (m, 1 H), 4.54–4.87 (m, 1 H), 5.56–6.40 (m, 1 H), 6.68–6.95 (m, 1 H), 7.25 (d, $J = 8.59$ Hz, 2 H), 7.63–7.77 (m, 3 H), 7.88 (d, $J = 7.41$ Hz, 1 H), 8.07 (d, $J = 7.81$ Hz, 1 H), 8.25 (br. s., 1 H), 8.30 (s, 1 H) 10.29 (br. s., 1 H). LC-MS: 100%, $m/z = 510.0$ [M + H]; HRMS [M + H] for $\text{C}_{29}\text{H}_{32}\text{N}_7\text{O}_2$, calcd, 510.2612; found, 510.2611.

(*R*)-3-(1-(1-Acryloylpiperidin-3-yl)-4-amino-1H-pyrazolo[3,4-*d*]pyrimidin-3-yl)-*N*-(4-isopropylphenyl)-*N*-methylbenzamide (54). **Step 1:** To a stirred solution of compound 28 (200 mg, 0.457 mmol,

1.0 equiv) in THF was added triethylamine (162 mg, 1.6 mmol, 3.5 equiv), 4-isopropyl-*N*-methylaniline (68 mg, 0.457 mmol, 1.0 equiv), and propylphosphonic anhydride (435 mg, 1.37 mmol, 3.0 equiv) at 0 °C. The reaction mixture was stirred at room temperature for 16 h. It was quenched with ice water and extracted with ethyl acetate (3 × 50 mL). The organic layer was washed with water (1 × 30 mL), brine (1 × 30 mL), dried over sodium sulfate, and was evaporated to dryness. The crude mass was purified by column chromatography (20% ethyl acetate in hexane) to afford the desired material **29b** as a brown solid (150 mg, 58%). ¹H NMR (400 MHz, CDCl₃): δ = 1.15 (d, 6H), 1.43 (s, 9H), 1.69 (d, 1H), 1.87 (s, 1H), 2.22–2.16 (m, 2H), 2.86–2.80 (m, 2H), 3.49 (s, 3H), 4.12–4.10 (m, 1H), 4.81 (s, 1H), 5.23 (s, 2H), 6.99 (d, 2H), 7.08 (d, 2H), 7.30 (s, 2H), 7.60 (s, 1H), 7.71 (s, 1H), 8.35 (s, 1H); LC-MS: *m/z* = 568.2 [M + H].

Step 2: To a stirred solution of **29b** (100 mg, 0.216 mmol, 1.0 equiv) in dioxane (1 mL) was added 4 N HCl in dioxane (7 mL) at 0 °C, and it was stirred at room temperature for 3 h. Then, the excess dioxane was evaporated. The reaction residue was triturated with *n*-pentane. The solid was collected by filtration and dried to afford the deprotected piperidine. The white solid (130 mg, 91%) was directly used for the next step as HCl salt. LC-MS: *m/z* = 470.0 [M + H].

Step 3: To a stirred solution of the deprotected piperidine (130 mg, 0.25 mmol, 1.0 equiv) in DMF (2 mL) was added BOP reagent (110.6 mg, 0.25 mmol, 1.0 equiv) followed by DIPEA (0.108 mL, 0.625 mmol, 2.5 equiv) and acrylic acid (19.9 mg, 0.276 mmol, 1.1 equiv). The reaction was stirred at room temperature for 10 min. Then, it was quenched with ice water and filtered. The residue was dissolved in ethyl acetate, dried over sodium sulfate, and was concentrated to dryness. The crude product was purified by prep-HPLC to afford final compound **54** as a white solid (30 mg, 24%). ¹H NMR (400 MHz, DMSO-*d*₆, 100 °C): δ = 1.12 (d, 6 H), 1.48–1.28 (m, 1 H), 1.68–1.62 (m, 1 H), 1.99–1.95 (m, 1 H), 2.33–2.15 (m, 1 H), 2.82 (q, 1 H), 3.17 (t, 1 H), 3.40 (s, 3 H), 3.50 (br s, 1 H), 4.11–4.08 (m, 1 H), 4.35 (br s, 1 H), 4.75–4.70 (m, 1 H), 5.63–5.61 (m, 1 H), 6.08–6.04 (m, 2 H), 6.40 (s, 2 H), 6.74–6.67 (m, 1 H), 7.14 (s, 4 H), 7.41–7.38 (m, 2 H), 7.59 (s, 2 H), 8.26 (s, 1 H). HPLC purity: 94.79%; HRMS [M + H] for C₃₀H₃₄N₇O₂, calcd, 524.2768; found, 524.2767.

(*R,E*)-3-(4-Amino-1-(1-but-2-enoyl)piperidin-3-yl)-1H-pyrazolo[3,4-*d*]pyrimidin-3-yl)-*N*-(4-isopropylphenyl)benzamide (**55**). By following a procedure similar to that for target **57**, the free piperidine prepared for the synthesis of **40** (75 mg, 0.16 mmol, 1.0 equiv) was converted into **55** (7 mg, 8%). ¹H NMR (400 MHz, DMSO-*d*₆): δ = 1.20 (d, *J* = 6.59 Hz, 6 H), 1.50–2.00 (m, 5 H), 2.13 (d, *J* = 8.79 Hz, 1 H), 2.22–2.36 (m, 1 H), 2.87 (dt, *J* = 13.73, 6.97 Hz, 1 H), 3.13–3.25 (m, 1 H), 4.01–4.41 (m, 2 H), 4.46–4.85 (m, 2 H), 6.25–6.83 (m, 2 H), 7.23 (d, *J* = 8.79 Hz, 2 H), 7.61–7.76 (m, 3 H), 7.86 (d, *J* = 7.47 Hz, 1 H), 8.05 (d, *J* = 7.91 Hz, 1 H), 8.23 (br. s., 1 H), 8.29 (br. s., 1 H), 10.27 (s, 1 H). LC-MS: 100%, *m/z* = 524.3 [M + H]; HRMS [M + H] for C₃₀H₃₄N₇O₂, calcd, 524.2768; found, 524.2769.

(*R*)-3-(4-Amino-1-(1-methacryloylpiperidin-3-yl)-1H-pyrazolo[3,4-*d*]pyrimidin-3-yl)-*N*-(4-isopropylphenyl)benzamide (**56**). By following a procedure similar to that for target **57**, the free piperidine prepared for the synthesis of **40** (75 mg, 0.16 mmol, 1.0 equiv) was converted into **56** (11 mg, 13%). ¹H NMR (600 MHz, DMSO-*d*₆): δ = 1.20 (d, *J* = 7.02 Hz, 6 H), 1.58–1.65 (m, 2 H), 1.85 (br. s., 3 H), 1.94 (d, *J* = 13.59 Hz, 2 H), 2.12–2.20 (m, 2 H), 2.31 (d, *J* = 8.77 Hz, 1 H), 2.87 (dt, *J* = 13.70, 6.96 Hz, 1 H), 4.73–4.82 (m, 1 H), 4.96–5.20 (m, 2 H), 7.22 (d, *J* = 8.33 Hz, 1 H), 7.65–7.72 (m, 3 H), 7.86 (d, *J* = 7.45 Hz, 1 H), 8.05 (d, *J* = 7.89 Hz, 1 H), 8.23 (s, 1 H), 8.28 (s, 1 H), 10.22 (s, 3 H). LC-MS: 100%, *m/z* = 524.3 [M + H]; HRMS [M + H] for C₃₀H₃₄N₇O₂, calcd, 524.2768; found, 524.2770.

(*R*)-3-(4-Amino-1-(1-(3-methylbut-2-enoyl)piperidin-3-yl)-1H-pyrazolo[3,4-*d*]pyrimidin-3-yl)-*N*-(4-isopropylphenyl)benzamide (**57**). To a cooled solution of the free piperidine prepared for the synthesis of **40** (75 mg, 0.16 mmol, 1.0 equiv) in dichloromethane (4 mL) at 0 °C was added triethylamine (0.115 mL, 0.825 mmol, 5.0 equiv). The reaction was stirred for 5 min resulting in a homogeneous solution. To the reaction was added a solution of 3-methylcrotonoyl chloride (0.018 mL, 0.165 mmol, 1.0 equiv) in dichloromethane (1 mL).

The reaction was stirred for 30 min. The reaction was judged complete by LC-MS and quenched with water and extracted with ethyl acetate. The organic layer was then concentrated and dissolved in DMSO. The crude product solution in DMSO was purified via prep-HPLC to provide the desired material (54 mg, 61%). ¹H NMR (600 MHz, DMSO-*d*₆): δ = 1.20 (d, *J* = 7.02 Hz, 6 H), 1.52–1.98 (m, 4 H), 2.10–2.35 (m, 1 H), 2.87 (dt, *J* = 13.59, 6.80 Hz, 1 H), 2.92–3.30 (m, 1 H), 3.58 (m, 6 H), 3.69–4.21 (m, 2 H), 4.48–4.77 (m, 1 H), 5.77–5.98 (m, 1 H), 7.22 (d, *J* = 8.77 Hz, 2 H), 7.67–7.72 (m, 3 H), 7.86 (d, *J* = 7.45 Hz, 1 H), 8.06 (d, *J* = 7.89 Hz, 1 H), 8.23 (br. s., 1 H), 8.32 (s, 1 H), 10.23 (s, 1 H). LC-MS: 100%, *m/z* = 538.3 [M + H]; HRMS [M + H] for C₃₁H₃₆N₇O₂, calcd, 538.2925; found, 538.2927.

(*R,E*)-3-(4-Amino-1-(1-(4-hydroxybut-2-enoyl)piperidin-3-yl)-1H-pyrazolo[3,4-*d*]pyrimidin-3-yl)-*N*-(4-isopropylphenyl)benzamide (**58**). By following a procedure similar to that for **62**, the free piperidine prepared for the synthesis of **40** (82 mg, 0.18 mmol, 1.0 equiv) was converted into **58** (46 mg, 48%). ¹H NMR (600 MHz, DMSO-*d*₆): δ = 0.65–0.81 (m, 6 H), 1.15 (br. s., 1 H), 1.48 (br. s., 1 H), 1.69 (d, *J* = 9.21 Hz, 1 H), 1.83 (d, *J* = 10.52 Hz, 1 H), 2.42 (dt, *J* = 14.03, 7.02 Hz, 1 H), 2.77 (br. s., 1 H), 3.21 (s, 2 H), 3.57–3.78 (m, 2 H), 4.07–4.37 (m, 1 H), 5.95–6.30 (m, 2 H), 6.77 (d, *J* = 8.33 Hz, 2 H), 7.14–7.30 (m, 3 H), 7.41 (d, *J* = 7.89 Hz, 1 H), 7.61 (d, *J* = 7.89 Hz, 1 H), 7.77 (s, 1 H), 7.88 (s, 1 H), 9.77 (s, 1 H). LC-MS: 100%, *m/z* = 540.3 [M + H]; HRMS [M + H] for C₃₀H₃₄N₇O₃, calcd, 540.2718; found, 540.2717.

(*R,E*)-3-(4-Amino-1-(1-(4-(methylamino)but-2-enoyl)piperidin-3-yl)-1H-pyrazolo[3,4-*d*]pyrimidin-3-yl)-*N*-(4-isopropylphenyl)benzamide (**59**). To a solution of the bromocrotonamide obtained in the synthesis of **61** (100 mg, 0.166 mmol, 1.0 equiv) in THF (10 mL) was added triethylamine (0.069 mL, 0.498 mmol, 3.0 equiv), methyl amine (0.830 mmol, 5.0 equiv), and potassium iodide (27.7 mg, 0.166 mmol, 1.0 equiv). The reaction was stirred at room temperature overnight in a sealed vial. The LC-MS of the reaction mixture showed completion of the reaction. The reaction was concentrated to dryness and diluted with DMSO, which was subjected to HPLC purification to provide the desired material **59** as a solid (2.9 mg, 3%). LC-MS: 99%, *m/z* = 553.2 [M + H];

(*R,E*)-3-(4-Amino-1-(1-(4-(piperazin-1-yl)but-2-enoyl)piperidin-3-yl)-1H-pyrazolo[3,4-*d*]pyrimidin-3-yl)-*N*-(4-isopropylphenyl)benzamide (**60**). To a solution of the Boc-protected piperazine intermediate (prepared analogously to **59**) (75 mg, 0.11, 1.0 equiv) in dichloromethane (0.5 mL) was added 4 N HCl in dioxane (0.265 mL, 1.06 mmol, 10.0 equiv), and the reaction was stirred overnight. LC-MS indicated the reaction was completed. The reaction was concentrated to a residue and diluted with DMSO and subjected to HPLC purification to provide the desired material as a solid (50 mg, 78%). ¹H NMR (600 MHz, DMSO-*d*₆): δ = 1.12–1.31 (m, 6 H), 1.59 (br. s., 2 H), 1.95 (br. s., 2 H), 2.09–2.35 (m, 6 H), 2.59–2.76 (m, 4 H), 2.83–3.17 (m, 4 H), 4.00–4.17 (m, 1 H), 4.50–4.83 (m, 1 H), 6.41–6.68 (m, 1 H), 7.23 (d, *J* = 8.33 Hz, 2 H), 7.58–7.76 (m, 3 H), 7.86 (d, *J* = 7.02 Hz, 1 H), 8.05 (d, *J* = 7.89 Hz, 1 H), 8.20–8.31 (m, 2 H), 10.23 (s, 1 H). LC-MS: 91%, *m/z* = 609.3 [M + H]; HRMS [M + Na] for C₃₄H₄₁N₉NaO₂, calcd, 630.3275; found, 630.3275.

(*R,E*)-3-(4-Amino-1-(1-(4-(2-aminoethyl)piperazin-1-yl)but-2-enoyl)piperidin-3-yl)-1H-pyrazolo[3,4-*d*]pyrimidin-3-yl)-*N*-(4-isopropylphenyl)benzamide (**61**). **Step 1:** To a cooled solution of the free piperidine prepared for the synthesis of **40** (500 mg, 1.10 mmol, 1.0 equiv) in dichloromethane (10 mL) at 0 °C was added triethylamine (0.305 mL, 2.20 mmol, 2.0 equiv). The reaction was stirred for 5 min resulting in a homogeneous solution. To the reaction was added (*E*)-4-bromobut-2-enoyl chloride (201 mg, 1.1 mmol, 1.0 equiv). The reaction was stirred for 1 h. The reaction was judged complete by LC-MS and quenched with water and extracted with ethyl acetate. The organic layer was then concentrated and purified via silica gel chromatography (50% ethyl acetate in heptane to 100%) to provide the desired product as a solid (325 mg, 49%). LC-MS: 96%, *m/z* = 602.2/604.2 [M + H].

Step 2: To a solution of the bromocrotonamide from the previous reaction (300 mg, 0.498 mmol, 1.0 equiv) in THF (10 mL) was added triethylamine (0.208 mL, 1.49 mmol, 3.0 equiv) followed by *tert*-butyl 2-(piperazin-1-yl)ethylcarbamate (114 mg, 0.498 mmol, 1.0 equiv).

The reaction was stirred overnight at room temperature. The reaction was judged complete by LC-MS and was concentrated under vacuum. The residue was purified via C18 reverse phase chromatography (5% acetonitrile in water (0.01% formic acid) to 95%) to provide the desired product as a white solid (231 mg, 62%). LC-MS: 99%, m/z = 751.3 [M + H].

Step 3: A solution of the Boc-protected material from the previous reaction (220 mg, 0.293 mmol, 1.0 equiv) in methanol (5 mL) was cooled to 0 °C, and 4 N HCl in dioxane (0.733 mL, 2.93 mmol, 10.0 equiv) was added. The reaction was stirred for 2 h at 0 °C and then at room temperature overnight. The reaction was judged complete by LC-MS, and the reaction was concentrated to the desired material as the HCl salt (200 mg, 99%). ¹H NMR (400 MHz, DMSO-*d*₆): δ = 1.22 (d, J = 7.02 Hz, 6 H), 1.54–2.37 (m, 6 H), 2.89 (dt, J = 13.76, 6.98 Hz, 1 H), 2.94–3.54 (m, 12 H), 3.71–3.98 (m, 2 H), 4.05–4.34 (m, 1 H), 4.57–4.94 (m, 2 H), 6.59–7.13 (m, 2 H), 7.25 (d, J = 8.59 Hz, 2 H), 7.69–7.79 (m, 3 H), 7.89 (d, J = 7.81 Hz, 1 H), 8.15–8.18 (m, 3 H), 8.26 (s, 1 H), 8.56–8.63 (m, 1 H), 10.29–10.42 (m, 1 H). LC-MS: 99%, m/z = 651.3 [M + H]; HRMS [M + H] for C₃₆H₄₇N₁₀O₂, calcd, 651.3878; found, 651.3874.

(R)-3-(4-Amino-1-(1-propiololylpiperidin-3-yl)-1H-pyrazolo[3,4-d]pyrimidin-3-yl)-N-(4-isopropylphenyl)benzamide (62). A solution of the free piperidine prepared for the synthesis of **40** (75 mg, 0.16 mmol, 1.0 equiv) and propargylic acid (17.3 mg, 0.247 mmol, 1.5 equiv) in DMF (0.8 mL) was cooled to 0 °C. To the solution was added DIPEA (0.086 mL, 0.495 mmol, 3.0 equiv) followed by BOP (109 mg, 0.247 mmol, 1.5 equiv). The reaction was stirred for 1 h, then allowed to warm to room temperature. The reaction was continued for 2 h at which point LC-MS indicated that the reaction was complete. The reaction was quenched with water and extracted with ethyl acetate. The organic layer was then concentrated and dissolved in DMSO. The crude product solution in DMSO was purified via prep-HPLC to provide the desired material (44 mg, 53%). ¹H NMR (600 MHz, DMSO-*d*₆): δ = 1.20 (d, J = 6.58 Hz, 6 H), 1.47–1.78 (m, 1 H), 1.84–2.34 (m, 3 H), 2.87 (dt, J = 13.70, 6.96 Hz, 1 H), 3.10–3.44 (m, 1 H), 3.27–3.46 (m, 1 H), 3.88 (dd, J = 13.15, 9.21 Hz, 1 H), 4.03–4.26 (m, 1 H), 4.30–4.49 (m, 1 H), 4.38–4.50 (m, 1 H), 4.69–5.00 (m, 1 H), 7.22 (d, J = 8.33 Hz, 2 H), 7.63–7.73 (m, 3 H), 7.88 (dd, J = 6.36, 1.53 Hz, 1 H), 8.07 (d, J = 7.89 Hz, 1 H), 8.24 (s, 1 H), 8.30–8.40 (m, 1 H), 10.22 (d, J = 8.33 Hz, 1 H). LC-MS: 94%, m/z = 508.1 [M + H]; HRMS [M + H] for C₂₉H₃₀N₇O₂, calcd, 508.2455; found, 508.2454.

(R)-3-(1-(1-Acryloylpiperidin-3-yl)-4-amino-1H-pyrazolo[3,4-d]pyrimidin-3-yl)-N-(4-isopropylphenyl)benzamide (63). By following a procedure similar to that for **62**, the free piperidine prepared for the synthesis of **40** (75 mg, 0.16 mmol, 1.0 equiv) was converted into **63** (45 mg, 53%). ¹H NMR (600 MHz, DMSO-*d*₆): δ = 1.15–1.25 (m, 6 H), 1.52–1.70 (m, 1 H), 1.87–2.04 (m, 3 H), 1.94–2.02 (m, 1 H), 2.17 (br. s., 1 H), 2.25–2.34 (m, 1 H), 2.87 (dt, J = 13.92, 6.85 Hz, 1 H), 3.33 (dd, J = 12.28, 10.52 Hz, 1 H), 3.85 (dd, J = 12.94, 8.99 Hz, 1 H), 4.01–4.24 (m, 1 H), 4.33–4.46 (m, 1 H), 4.68–4.88 (m, 1 H), 7.23 (d, J = 7.89 Hz, 2 H), 7.66–7.74 (m, 3 H), 7.87 (d, J = 7.45 Hz, 1 H), 8.07 (dd, J = 7.67, 1.10 Hz, 1 H), 8.24 (d, J = 1.75 Hz, 1 H), 8.35 (d, J = 9.65 Hz, 1 H), 10.22 (d, J = 3.51 Hz, 1 H). LC-MS: 100%, m/z = 522.2 [M + H]; HRMS [M + H] for C₃₀H₃₂N₇O₂, calcd, 522.2612; found, 522.2616.

(R)-3-(4-Amino-1-(1-cyanopiperidin-3-yl)-1H-pyrazolo[3,4-d]pyrimidin-3-yl)-N-(4-isopropylphenyl)benzamide (64). A solution of the free piperidine prepared for the synthesis of **40** (50 mg, 0.11 mmol, 1.0 equiv) and cesium carbonate (143 mg, 0.440 mmol, 4.0 equiv) in DMF (2 mL) was cooled to 0 °C. To the solution was added cyanogen bromide (0.073 mL, 0.220 mmol, 2.0 equiv), and the reaction was stirred for 30 min, then allowed to warm to room temperature. The reaction was continued for 30 min at which point LC-MS indicated the reaction was complete. The reaction was quenched with water and extracted with ethyl acetate. The organic layer was then concentrated and dissolved in DMSO. The crude product solution in DMSO was purified via prep-HPLC to provide the desired material (29 mg, 55%). ¹H NMR (600 MHz, DMSO-*d*₆): δ = 1.20 (d, J = 7.02 Hz, 6 H) 1.83 (br. s., 1 H) 1.91 (d, J = 3.51 Hz, 1 H) 2.13 (d, J = 3.51 Hz, 1 H) 2.20

(d, J = 3.07 Hz, 1 H) 2.84–2.92 (m, 1 H) 3.18 (dd, J = 11.62, 9.87 Hz, 1 H) 3.40 (d, J = 12.72 Hz, 1 H) 3.56 (dd, J = 12.50, 10.30 Hz, 1 H) 3.65 (dd, J = 12.28, 4.39 Hz, 1 H) 4.86–4.95 (m, 1 H) 7.22 (d, J = 8.77 Hz, 2 H) 7.63–7.72 (m, 3 H) 7.87 (d, J = 7.89 Hz, 1 H) 8.06 (d, J = 7.89 Hz, 1 H) 8.19–8.26 (m, 1 H) 8.30 (s, 1 H) 10.22 (s, 1 H). LC-MS: 97%, m/z = 481.2 [M + H]; HRMS [M + H] for C₂₇H₂₉N₉O, calcd, 481.2459; found, 481.2460.

(R)-3-(1-(1-Acryloylpiperidin-3-yl)-4-amino-1H-pyrazolo[3,4-d]pyrimidin-3-yl)-N-benzamide (65). **Step 1:** To a stirred solution of compound **28** (150 mg, 0.342 mmol, 1.0 equiv) in DMF (3 mL) was added DIPEA (132.4 mg, 1.026 mmol, 3.0 equiv), HATU (143 mg, 0.376 mmol, 1.1 equiv), and benzylamine (36.6 mg, 0.342 mmol, 1.0 equiv) at 0 °C. The reaction mixture was stirred at room temperature for 4 h. The reaction mixture was quenched with ice water and was extracted with ethyl acetate (3 × 50 mL). The organic layer was washed with water (2 × 20 mL) followed by brine (1 × 20 mL), dried over sodium sulfate, and was evaporated to dryness. The crude material was purified by column chromatography (30% ethyl acetate in hexane) to afford compound **29a** as an off-white solid (125 mg, 69%). ¹H NMR (400 MHz, DMSO-*d*₆): δ = 1.42 (s, 9 H), 1.69–1.66 (m, 2 H), 2.29–2.26 (m, 2 H), 3.60–3.20 (m, 2 H), 4.08 (m, 1 H), 4.40–4.10 (m, 1 H), 4.66 (d, 2 H), 4.82 (m, 1 H), 7.36–7.31 (m, 5 H), 7.60 (t, 1 H), 7.82 (t, 1 H), 7.87 (d, 1 H), 8.11 (s, 1 H), 8.34 (s, 1 H). LC-MS: m/z = 528.4 [M + H].

Step 2: To a stirred solution of compound **29a** (100 mg, 0.216 mmol, 1.0 equiv) in dioxane (1 mL) was added 4 N HCl in dioxane (7 mL) at 0 °C, and it was stirred at room temperature for 3 h. Then, the solvent was evaporated, and the residue was triturated with *n*-pentane. The solid was collected by filtration and was dried under vacuum to afford the deprotected piperidine. This off-white solid (100 mg, 84%) was directly used for the next step as HCl salt. LC-MS (M + H): 428.6.

Step 3: To a stirred solution of the deprotected piperidine (100 mg, 0.216 mmol, 1.0 equiv) in DMF (2 mL) was added BOP reagent (95.4 mg, 0.216 mmol, 1.0 equiv) followed by DIPEA (0.093 mL, 0.54 mmol, 2.5 equiv) and acrylic acid (17.1 mg, 0.237 mmol, 1.1 equiv) at 0 °C. The reaction mixture was stirred at room temperature for 15 min. The reaction was quenched with ice water and filtered. The residue was dissolved in ethyl acetate, dried over sodium sulfate, and was concentrated. The crude mass was purified by prep-HPLC to afford final compound **65** as a white solid (19 mg, 21%). ¹H NMR (400 MHz, DMSO-*d*₆): δ = 1.68–1.62 (m, 1 H), 1.99–1.95 (m, 1 H), 2.38–2.18 (m, 1 H), 3.20–3.14 (m, 1 H), 3.55 (s, 1 H), 4.12–4.08 (m, 1 H) 4.42–4.39 (m, 1 H), 4.50 (d, 2 H), 4.79–4.74 (m, 1 H), 5.66–5.60 (m, 1 H), 6.08–6.03 (m, 1 H), 6.53 (s, 2 H), 6.74–6.67 (m, 1H), 7.38–7.22 (m, 5 H), 7.63 (t, 1 H), 7.81 (d, 1 H), 8.0 (d, 1 H), 8.19 (s, 1 H), 8.28 (s, 1 H), 8.79 (s, 1 H). HPLC purity: 97.09%; HRMS [M + H] for C₂₇H₂₈N₇O₂, calcd, 482.2299; found, 482.2302.

(R)-3-(1-(1-Acetylpiperidin-3-yl)-4-amino-1H-pyrazolo[3,4-d]pyrimidin-3-yl)-N-benzylbenzamide (66). To a stirred solution of the deprotected piperidine prepared for the synthesis of compound **65** (200 mg, 0.562 mmol) in dichloromethane (10 mL) was added triethylamine (0.313 mL, 2.248 mmol) and acetyl chloride (0.036 mL, 0.505 mmol) at 0 °C. The reaction mixture was allowed to stir at the same temperature for 2 h. The reaction mixture was diluted with dichloromethane (5 mL), and the organic layer was washed with water (2 × 10 mL) followed by brine (1 × 10 mL), dried over sodium sulfate, and was evaporated to dryness. The crude mass was purified by column chromatography (3% methanol in dichloromethane) to afford the desired material **66** as a white solid (120 mg, 45%). ¹H NMR (400 MHz, DMSO-*d*₆): δ = 1.58 (m, 1 H), 1.67 (m, 1 H), 1.97 (s, 3 H), 2.07 (m, 1 H), 2.23 (m, 1 H), 2.79–3.17 (m, 2 H), 3.60–3.85 (m, 1 H), 3.98–4.23 (m, 1 H), 4.51 (m, 2 H), 4.62–4.80 (m, 1 H), 7.26 (m, 1 H), 7.34 (d, 4 H), 7.64 (t, 1 H), 7.81 (d, 1 H), 8.00 (d, 1 H), 8.19 (s, 1 H), 8.28 (d, 1 H), 9.15 (m, 1 H); HPLC purity = 96.13%; HRMS [M + H] for C₂₆H₂₈N₇O₂, calcd, 470.2299; found, 470.2302.

(R)-3-(1-(1-Acetylpiperidin-3-yl)-4-amino-1H-pyrazolo[3,4-d]pyrimidin-3-yl)-N-(4-methylbenzyl)benzamide (68). **Step 1:** To a stirred solution of **28** (300 mg, 0.684 mmol) in dichloromethane (10 mL) was added 4-methylbenzyl amine (0.104 mL, 0.820 mmol)

and DIPEA (0.226 mL, 1.368 mmol) followed by the addition of PyBOP (534 mg, 1.026 mmol). The reaction mixture was allowed to stir at room temperature for 18 h. The reaction mixture was diluted with dichloromethane (15 mL). The organic layer was washed with water (2 × 10 mL) followed by brine (1 × 10 mL), dried over sodium sulfate, and was evaporated to dryness. The residue was purified by column chromatography (100% ethyl acetate) to afford compound 30 as a white solid (349 mg, 94%). ¹H NMR (400 MHz, DMSO-*d*₆): δ = 1.34 (s, 9H), 1.57 (m, 1H), 1.85 (m, 1H), 2.18 (m, 1H), 2.31 (s, 3H), 3.13 (m, 1H), 3.30 (m, 1H), 3.62 (m, 1H), 3.85 (m, 1H), 4.46 (d, 2H), 4.69 (m, 1H), 7.13 (d, 2H), 7.22 (d, 2H), 7.63 (m, 1H), 7.79 (d, 1H), 7.98 (d, 1H), 8.17 (s, 1H), 8.27 (s, 1H), 9.09 (m, 1H); LC-MS *m/z* = 542.2 [M + H].

Step 2: To a stirred solution of compound 29 (349 mg, 0.644 mmol) in dioxane (2 mL) was added 4 N HCl in dioxane (10 mL) at 0 °C. The reaction mixture was allowed to stir at room temperature for 1 h. The reaction mixture was evaporated to dryness and was triturated with diethyl ether to afford the HCl salt of the deprotected piperidine as a white solid (280 mg). ¹H NMR (400 MHz, DMSO-*d*₆): δ = 1.95 (s, 2 H), 2.17 (m, 2 H), 2.49 (s, 3 H), 3.11 (m, 1 H), 3.30 (m, 1 H), 3.44 (m, 1 H), 3.60 (m, 1 H), 4.46 (d, 2 H), 5.22 (m, 1 H), 7.13 (d, 2 H), 7.22 (d, 2 H), 7.66 (t, 1 H), 7.82 (d, 1 H), 8.06 (d, 1 H), 8.22 (s, 1 H), 8.52 (s, 1 H), 9.18–9.38 (m, 3 H); LC-MS *m/z* = 442.2 [M + H].

Step 3: To a stirred solution of the deprotected piperidine (280 mg, 0.634 mmol) in dichloromethane (10 mL) was added triethylamine (0.354 mL, 2.539 mmol) and acetyl chloride (0.04 mL, 0.571 mmol) at 0 °C, and the reaction mixture was allowed to stir at the same temperature for 2 h. The reaction mixture was diluted with dichloromethane (5 mL), and the organic layer was washed with water (2 × 10 mL) followed by brine (1 × 10 mL), dried over sodium sulfate, and was evaporated to dryness. The crude mass was purified by column chromatography (3% methanol in dichloromethane) to afford compound 68 as a white solid (120 mg, 45%). ¹H NMR (400 MHz, DMSO-*d*₆): δ = 1.52 (m, 1 H), 1.66 (m, 1 H), 1.97 (s, 3 H), 2.11 (m, 1 H), 2.27 (m, 4 H), 2.79–3.17 (m, 2 H), 3.60–3.80 (m, 1 H), 3.99–4.23 (m, 1 H), 4.51–4.54 (dd, 2 H), 4.75–4.80 (m, 1 H), 7.13 (d, 2 H), 7.22 (d, 2 H), 7.63 (t, 1 H), 7.80 (d, 1 H), 7.98 (d, 1 H), 8.18 (s, 1 H), 8.28 (d, 1 H), 9.11 (m, 1 H); HPLC purity = 97.65%; HRMS [M + H] for C₂₇H₃₀N₇O₂, calcd, 484.2455; found, 484.2458.

3-(1-(1-Acetylpiperidin-3-yl)-4-amino-1H-pyrazolo[3,4-d]pyrimidin-3-yl)-N-(4-isopropylphenyl)benzamide (69). Triethylamine (152 mg, 1.5 mmol) followed by acetyl chloride (43 mg, 550 μmol) was added to the suspension of 3-{4-amino-3-[3-(4-isopropylphenylcarbamoyl)phenyl]pyrazolo[3,4-d]pyrimidin-1-yl}piperidinium chloride (246 mg, 500 μmol) in dichloromethane (1.5 mL) at 0 °C while stirring. The cooling bath was removed, and the mixture was stirred for 30 min. The mixture was then directly purified by column chromatography (0% methanol in dichloromethane to 7%) to afford 69 (183 mg, 73%) as a colorless glass. ¹H NMR (400 MHz, DMSO-*d*₆): δ = 0.96–1.34 (m, 6 H), 1.40–1.92 (m, 2 H), 1.96–2.08 (m, 3 H), 2.07–2.39 (m, 2 H), 2.69–3.21 (m, 3 H), 3.56–4.58 (m, 2 H), 4.58–4.85 (m, 1 H), 7.22 (d, *J* = 8.79 Hz, 2 H), 7.57–7.73 (m, 3 H), 7.86 (d, *J* = 8.05 Hz, 1 H), 8.04 (d, *J* = 8.05 Hz, 1 H), 8.22 (d, *J* = 1.46 Hz, 1 H), 8.25–8.34 (m, 1 H), 10.27 (s, 1 H). LC-MS: 99%, *m/z* = 498.3; HRMS [M + H] for C₂₈H₃₂N₇O₂, calcd, 498.2612; found, 498.2617.

3-(1-(1-Acetylpiperidin-3-yl)-4-amino-1H-pyrazolo[3,4-d]pyrimidin-3-yl)-N-(3-tert-butylphenyl)benzamide (70). Triethylamine (152 mg, 1.5 mmol, 3.0 equiv) followed by acetyl chloride (43 mg, 550 μmol, 1.1 equiv) was added to the suspension of 3-{4-amino-3-[3-(3-tert-butylphenylcarbamoyl)phenyl]pyrazolo[3,4-d]pyrimidin-1-yl}piperidinium chloride (253 mg, 500 μmol, 1.0 equiv) in dichloromethane (1.5 mL) at 0 °C while stirring. The cooling bath was removed, and the mixture was stirred for 30 min. The mixture was then directly purified by column chromatography (0% methanol in dichloromethane to 7%) to afford 71 (220 mg, 86%) as a colorless glass. ¹H NMR (400 MHz, DMSO-*d*₆): δ = 1.23–1.38 (m, 9 H), 7.15 (d, *J* = 7.32 Hz, 1 H), 7.29 (t, *J* = 8.05 Hz, 1 H), 7.61–7.76 (m, 1 H), 7.80 (br. s., 2 H), 7.88 (d, *J* = 8.05 Hz, 1 H), 8.07 (d, *J* = 7.32 Hz, 1 H),

8.21–8.39 (m, 1 H), 10.28 (s, 2 H). LC-MS: 99%, *m/z* = 512.3; HRMS [M + H] for C₂₉H₃₄N₇O₂, calcd, 512.2768; found, 512.2768.

(R)-3-(1-(1-Acetylpiperidin-3-yl)-4-amino-1H-pyrazolo[3,4-d]pyrimidin-3-yl)-N-(4-tert-butylbenzyl)benzamide (71). **Step 1:** To a stirred solution of acid compound 28 (300 mg, 0.684 mmol) in dichloromethane (10 mL) was added *tert*-butylbenzylamine (0.144 mL, 0.820 mmol) and DIPEA (0.226 mL, 1.368 mmol), followed by the addition of PyBOP (534 mg, 1.026 mmol), and the reaction mixture was allowed to stir at room temperature for 18 h. The reaction mixture was diluted with dichloromethane (15 mL). The organic layer was washed with water (2 × 10 mL) followed by brine (1 × 10 mL), dried over sodium sulfate, and was evaporated to dryness. The crude mass was purified by column chromatography (100% ethyl acetate) to afford compound 30 as an off-white solid (368 mg, 92%). ¹H NMR (400 MHz, DMSO-*d*₆): δ = 1.26–1.34 (m, 18 H), 1.56 (m, 1 H), 1.89 (m, 1 H), 2.09 (m, 1 H), 2.22 (m, 1 H), 2.96 (m, 1 H), 3.30–3.40 (m, 2 H), 3.86 (m, 1 H), 4.46 (d, 2 H), 4.69 (m, 1 H), 7.27 (d, 2 H), 7.35 (d, 2 H), 7.63 (t, 1 H), 7.80 (d, 1 H), 7.98 (d, 1 H), 8.18 (s, 1 H), 8.27 (s, 1 H), 9.09 (m, 1 H); LC-MS *m/z* = 584.4 [M + H].

Step 2: To a stirred solution of compound 29 (368 mg, 0.630 mmol) in dioxane (2 mL) was added 4 N HCl in dioxane (10 mL) at 0 °C. The reaction mixture was allowed to stir at room temperature for 1 h. The reaction mixture was evaporated to dryness and was triturated with diethyl ether to afford the deprotected piperidine as a white solid (300 mg). ¹H NMR (400 MHz, DMSO-*d*₆, 100 °C): δ = 1.25 (s, 9 H), 1.98 (m, 2 H), 2.14 (m, 2 H), 3.01 (m, 2 H), 3.30 (m, 1 H), 3.50 (m, 1 H), 4.47 (d, 2 H), 5.23 (m, 1 H), 7.26 (d, 2 H), 7.35 (d, 2 H), 7.66 (t, 1 H), 7.82 (d, 1 H), 8.07 (d, 1 H), 8.23 (s, 1 H), 8.57 (s, 1 H), 9.20–9.45 (m, 3 H); LC-MS = 484.2 [M + H].

Step 3: To a stirred solution of the deprotected piperidine (300 mg, 0.621 mmol) in dichloromethane (10 mL) was added triethylamine (0.346 mL, 2.484 mmol) and acetyl chloride (0.04 mL, 0.559 mmol) at 0 °C, and the reaction mixture was allowed to stir at the same temperature for 2 h. The reaction mixture was diluted with dichloromethane (5 mL), and the organic layer was washed with water (2 × 10 mL) followed by brine (1 × 10 mL), dried over sodium sulfate, and was evaporated to dryness. The crude mass was purified by column chromatography (3% methanol in dichloromethane) to afford 71 as a white solid (140 mg, 43%). ¹H NMR (400 MHz, DMSO-*d*₆): δ = 1.28 (s, 9H), 1.67 (m, 1H), 1.84 (m, 1H), 1.97 (s, 3H), 2.07 (m, 1H), 2.23 (m, 1H), 2.32 (m, 1H), 2.79–3.17 (m, 2H), 3.60–3.86 (m, 1H), 3.99–4.23 (m, 1H), 4.50–4.54 (m, 2H), 4.75–4.80 (m, 1H), 7.25 (d, 2H), 7.63 (d, 2H), 7.63 (t, 1H), 7.80 (d, 1H), 7.99 (d, 1H), 8.19 (s, 1H), 8.28 (d, 1H), 9.11 (m, 1H); HPLC purity = 99.02%; HRMS [M + H] for C₃₀H₃₆N₇O₂, calcd, 526.2925; found, 526.2926.

Amide Library. **Step 1:** A 0.2 M solution of acid template in anhydrous DMF was prepared (solution A), and a 0.2 M solution of amine monomers in anhydrous DMF was prepared (solution B). Solution A (625 μL (125 μmol)) was added to each reaction vial followed by 625 μL (1 equiv, 125 μmol) of solution B. HATU (125 μmol (1 equiv, 48 mg) was dispensed to each vial followed by DIPEA (125 μmol, 1.5 equiv, 22 μL). Reaction vials were shaken for 16 h at 60 °C and checked by LC-MS. Reaction mixtures were evaporated in a thermo explorer (2 h, 5 Torr, and 45 °C). Each residue was dissolved in ethyl acetate (5 mL) and washed with water (1 × 3 mL) and brine (1 × 3 mL). The organic part was dried over anhydrous sodium sulfate and evaporated under reduced pressure.

Step 2: Each residue obtained after step 1 was dissolved in 500 μL of 1,4-dioxane, transferred to reaction vials, and cooled to 0 °C. 1,4-Dioxane-HCl (1 M, 500 μL) was added to each reaction vial and stirred at 25 °C for 16 h. The solvent was evaporated under reduced pressure and azeotroped with toluene. Residues obtained were used in step 3 without further purification.

Step 3: To a solution of acrylic acid (250 mg, 3.5 mmol) in DCM (20 mL) was added thionyl chloride (1.5 equiv, 5.2 mmol, 0.38 mL). The reaction mixture was heated at 40 °C for 4 h, and half of the total volume of DCM was evaporated. The amine was dissolved in 1 mL of DCM, and 5 equiv of TEA (70 μL) was added to each reaction vial. The acryloyl chloride solution (1.5 equiv, 5.2 mmol, 0.38 mL) was slowly added to the solution of amine and TEA in DCM at 0 °C.

Reaction vials were stirred at 0 °C for 10–15 min after which it was quenched with ice. The solvent was evaporated. DMSO (1.0 mL) was added to the crude products. Ten microliters of the DMSO solution was diluted to 200 μ L with DMSO for QC analysis, and the remaining amount was submitted for prep-HPLC purification on Waters Auto-purification System (column, Luna Phenyl Hexyl (21 \times 150 mm, 10 μ m); mobile phase, A, 10 mM ammonium acetate in water, and B, acetonitrile; $T = 0$; flow = 20; A = 90%; B = 10%; $T = 3$; flow = 20; A = 75%; B = 25%; $T = 18$; flow = 20; A = 35%; B = 65%). Purified fractions were collected in bar coded test tubes and evaporated in a thermo explorer (40 °C, 15 Torr, 16 h). Each of the compounds were then dissolved in ethanol (1.6 mL) and transferred to 2 dram glass vials. Finally, they were dried in a Genevac first for 1 h (40 °C, 10 mbar) and then for 12 h (40 °C, 0 mbar). Weights were taken using a Mettler Balance. These compounds were then dissolved in calculated amounts of DMSO to prepare 30 mM solutions. Eight μ L was removed for final QC analysis (diluted with 150 μ L DMSO) on an analytical LC/MS. QC reports were generated to check the identity and purity of each compound.

- 30: LC-MS 83.9%, 1.73 min, $m/z = 536.35$ [M + H].
31: LC-MS 100%, 1.72 min, $m/z = 536.30$ [M + H].
32: LC-MS 100%, 1.56 min, $m/z = 498.27$ [M + H]; HRMS [M + H] for $C_{27}H_{28}N_7O_3$, calcd, 498.2248; found, 498.2249.
33: LC-MS 100%, 1.61 min, $m/z = 498.33$ [M + H]; HRMS [M + H] for $C_{27}H_{28}N_7O_3$, calcd, 498.2248; found, 498.2246.
34: LC-MS 100%, 1.61 min, $m/z = 486.31$ [M + H]; HRMS [M + H] for $C_{26}H_{25}FN_7O_2$, calcd, 486.2048; found, 486.2051.
35: LC-MS 97.7%, 1.66 min, $m/z = 504.08$ [M + H]; HRMS [M + H] for $C_{26}H_{24}N_7O_2$, calcd, 504.1954; found, 504.1957.
37: LC-MS 100%, 1.57 min, $m/z = 504.22$ [M + H]; HRMS [M + H] for $C_{26}H_{24}N_7O_2$, calcd, 504.1954; found, 504.1956.
38: LC-MS 94.1%, 1.58 min, $m/z = 487.29$ [M + H].
41 (PF-06465469):⁴³ LC-MS 95.1%, 1.79 min, $m/z = 524.28$ [M + H]; HRMS [M + H] for $C_{30}H_{34}N_7O_2$, calcd, 524.2768; found, 524.2771.
43: LC-MS 86.5%, 1.67 min, $m/z = 550.21$ [M + H].
44: LC-MS 100%, 1.54 min, $m/z = 507.33$ [M + H]; HRMS [M + H] for $C_{28}H_{27}N_8O_2$, calcd, 507.2251; found, 507.2255.
45: LC-MS 100%, 1.56 min, $m/z = 551.09$ [M + H]; HRMS [M + H] for $C_{27}H_{26}F_3N_8O_2$, calcd, 551.2125; found, 551.2128.
46: LC-MS 93.6%, 1.56 min, $m/z = 500.22$ [M + H]; HRMS [M + H] for $C_{27}H_{27}FN_7O_2$, calcd, 500.2205; found, 500.2205.
47: LC-MS 100%, 1.57 min, $m/z = 512.24$ [M + H]; HRMS [M + H] for $C_{28}H_{30}N_7O_3$, calcd, 512.2405; found, 512.2408.
48: LC-MS 91.8%, 1.62 min, $m/z = 514.29$ [M + H].
50: LC-MS 94.4%, 1.58 min, $m/z = 462.27$ [M + H]; HRMS [M + H] for $C_{25}H_{32}N_7O_2$, calcd, 462.2612; found, 462.2616.
51: LC-MS 97.0%, 1.50 min, $m/z = 474.18$ [M + H]; HRMS [M + H] for $C_{22}H_{23}F_3N_7O_2$, calcd, 474.1860; found, 474.1865.
67: LC-MS 96.5%, 1.63 min, $m/z = 496.26$ [M + H]; HRMS [M + H] for $C_{28}H_{30}N_7O_2$, calcd, 496.2455; found, 496.2458.

■ ASSOCIATED CONTENT

● Supporting Information

Assay details, electrophilicity calculations, and ¹H NMR spectra. This material is available free of charge via the Internet at <http://pubs.acs.org>.

Accession Codes

Coordinates of the Itk crystal structures have been deposited in the Protein Data Bank for compound 40 (4HCU), compound 52 (4HCT), and compound 53 (4HCV).

■ AUTHOR INFORMATION

Corresponding Author

*Tel: +1 617 665 5602. Fax: +1 617 665 5682. E-mail: christoph.zapf@pfizer.com.

Notes

The authors declare no competing financial interest.

■ ACKNOWLEDGMENTS

We thank Mark Schnute, Atli Thorarensen, Suvit Thaisrivongs, and Kyri Dunussi-Joannopoulos for stimulating discussions and support for the project.

■ ABBREVIATIONS USED

Itk, interleukin-2 inducible T cell kinase; IP1, inositol mono-phosphate; hWB, human whole blood; TCR, T cell receptor; BTK, Bruton's tyrosine kinase; PLC γ 1, phospholipase C, gamma 1; IP3, inositol trisphosphate; IL-2, interleukin 2; APC, antigen-presenting cell; KO, knockout; OVA, ovalbumin; siRNA, small interfering RNA; HATU, *O*-(7-azabenzotriazol-1-yl)-*N,N,N',N'*-tetramethyluronium hexafluorophosphate; μ M, micromolar; ADME, absorption, distribution, metabolism, and excretion; hERG, human ether-à-go-go-related gene; HLM, human liver microsome

■ REFERENCES

- (1) Iyer, A. S.; August, A. The Tec family kinase, IL-2-inducible T cell kinase, differentially controls mast cell responses. *J. Immunol.* **2008**, *180*, 7869–7877.
- (2) Andreotti, A. H.; Schwartzberg, P. L.; Joseph, R. E.; Berg, L. J. T-cell signaling regulated by the Tec family kinase, Itk. *Cold Spring Harbor Perspect. Biol.* **2010**, *2*, a002287.
- (3) Berg, L. J.; Finkelstein, L. D.; Lucas, J. A.; Schwartzberg, P. L. Tec family kinases in T lymphocyte development and function. *Annu. Rev. Immunol.* **2005**, *23*, 549–600.
- (4) Burbach, B. J.; Medeiros, R. B.; Mueller, K. L.; Shimizu, Y. T-cell receptor signaling to integrins. *Immunol. Rev.* **2007**, *218*, 65–81.
- (5) Sahu, N.; Mueller, C.; Fischer, A.; August, A. Differential sensitivity to Itk kinase signals for T helper 2 cytokine production and chemokine-mediated migration. *J. Immunol.* **2008**, *180*, 3833–3838.
- (6) Kosaka, Y.; Felices, M.; Berg, L. J. Itk and Th2 responses: action but no reaction. *Trends Immunol.* **2006**, *27*, 453–460.
- (7) Au-Yeung, B. B.; Katzman, S. D.; Fowell, D. J. Cutting edge: Itk-dependent signals required for CD4⁺ T cells to exert, but not gain, Th2 effector function. *J. Immunol.* **2006**, *176*, 3895–3899.
- (8) Gomez-Rodriguez, J.; Sahu, N.; Handon, R.; Davidson, T. S.; Anderson, S. M.; Kirby, M. R.; August, A.; Schwartzberg, P. L. Differential expression of interleukin-17A and -17F is coupled to T cell receptor signaling via inducible T cell kinase. *Immunity* **2009**, *31*, 587–597.
- (9) Takesono, A.; Horai, R.; Mandai, M.; Dombroski, D.; Schwartzberg, P. L. Requirement for Tec kinases in chemokine-induced migration and activation of Cdc42 and Rac. *Curr. Biol.* **2004**, *14*, 917–922.
- (10) Fischer, A. M.; Mercer, J. C.; Iyer, A.; Ragin, M. J.; August, A. Regulation of CXC chemokine receptor 4-mediated migration by the Tec family tyrosine kinase ITK. *J. Biol. Chem.* **2004**, *279*, 29816–29820.
- (11) Readinger, J. A.; Schiralli, G. M.; Jiang, J. K.; Thomas, C. J.; August, A.; Henderson, A. J.; Schwartzberg, P. L. Selective targeting of ITK blocks multiple steps of HIV replication. *Proc. Natl. Acad. Sci. U.S.A.* **2008**, *105*, 6684–6689.
- (12) Lin, T. A.; McIntyre, K. W.; Das, J.; Liu, C.; O'Day, K. D.; Penhallow, B.; Hung, C. Y.; Whitney, G. S.; Shuster, D. J.; Yang, X.; Townsend, R.; Postelnek, J.; Spergel, S. H.; Lin, J.; Moquin, R. V.; Furch, J. A.; Kamath, A. V.; Zhang, H.; Marathe, P. H.; Perez-Villar, J. J.; Doweiko, A.; Killar, L.; Dodd, J. H.; Barrish, J. C.; Wityak, J.; Kanner, S. B. Selective Itk inhibitors block T-cell activation and murine lung inflammation. *Biochemistry* **2004**, *43*, 11056–11062.
- (13) Das, J.; Furch, J. A.; Liu, C.; Moquin, R. V.; Lin, J.; Spergel, S. H.; McIntyre, K. W.; Shuster, D. J.; O'Day, K. D.; Penhallow, B.; Hung, C. Y.; Doweiko, A. M.; Kamath, A.; Zhang, H.; Marathe, P.; Kanner, S. B.; Lin, T. A.; Dodd, J. H.; Barrish, J. C.; Wityak, J.

Discovery and SAR of 2-amino-5-(thioaryl)thiazoles as potent and selective Itk inhibitors. *Bioorg. Med. Chem. Lett.* **2006**, *16*, 3706–3712.

(14) Kashem, M. A.; Nelson, R. M.; Yingling, J. D.; Pullen, S. S.; Prokopowicz, A. S., 3rd; Jones, J. W.; Wolak, J. P.; Rogers, G. R.; Morelock, M. M.; Snow, R. J.; Homon, C. A.; Jakes, S. Three mechanistically distinct kinase assays compared: Measurement of intrinsic ATPase activity identified the most comprehensive set of ITK inhibitors. *J. Biomol. Screening* **2007**, *12*, 70–83.

(15) Winters, M. P.; Robinson, D. J.; Khine, H. H.; Pullen, S. S.; Woska, J. R., Jr.; Raymond, E. L.; Sellati, R.; Cywin, C. L.; Snow, R. J.; Kashem, M. A.; Wolak, J. P.; King, J.; Kaplita, P. V.; Liu, L. H.; Farrell, T. M.; Desjarlais, R.; Roth, G. P.; Takahashi, H.; Moriarty, K. J. 5-Aminomethyl-1H-benzimidazoles as orally active inhibitors of inducible T-cell kinase (Itk). *Bioorg. Med. Chem. Lett.* **2008**, *18*, 5541–5544.

(16) Snow, R. J.; Abeywardane, A.; Campbell, S.; Lord, J.; Kashem, M. A.; Khine, H. H.; King, J.; Kowalski, J. A.; Pullen, S. S.; Roma, T.; Roth, G. P.; Sarko, C. R.; Wilson, N. S.; Winters, M. P.; Wolak, J. P.; Cywin, C. L. Hit-to-lead studies on benzimidazole inhibitors of ITK: discovery of a novel class of kinase inhibitors. *Bioorg. Med. Chem. Lett.* **2007**, *17*, 3660–3665.

(17) Moriarty, K. J.; Takahashi, H.; Pullen, S. S.; Khine, H. H.; Sallati, R. H.; Raymond, E. L.; Woska, J. R., Jr.; Jeanfavre, D. D.; Roth, G. P.; Winters, M. P.; Qiao, L.; Ryan, D.; Desjarlais, R.; Robinson, D.; Wilson, M.; Bobko, M.; Cook, B. N.; Lo, H. Y.; Nemoto, P. A.; Kashem, M. A.; Wolak, J. P.; White, A.; Magolda, R. L.; Tomczuk, B. Discovery, SAR and X-ray structure of 1H-benzimidazole-5-carboxylic acid cyclohexyl-methyl-amides as inhibitors of inducible T-cell kinase (Itk). *Bioorg. Med. Chem. Lett.* **2008**, *18*, 5545–5549.

(18) Cook, B. N.; Bentzien, J.; White, A.; Nemoto, P. A.; Wang, J.; Man, C. C.; Soleymanzadeh, F.; Khine, H. H.; Kashem, M. A.; Kugler, S. Z., Jr.; Wolak, J. P.; Roth, G. P.; De Lombaert, S.; Pullen, S. S.; Takahashi, H. Discovery of potent inhibitors of interleukin-2 inducible T-cell kinase (ITK) through structure-based drug design. *Bioorg. Med. Chem. Lett.* **2009**, *19*, 773–777.

(19) Riether, D.; Zindell, R.; Kowalski, J. A.; Cook, B. N.; Bentzien, J.; Lombaert, S. D.; Thomson, D.; Kugler, S. Z., Jr.; Skow, D.; Martin, L. S.; Raymond, E. L.; Khine, H. H.; O'Shea, K.; Woska, J. R., Jr.; Jeanfavre, D.; Sellati, R.; Ralph, K. L.; Ahlberg, J.; Labissiere, G.; Kashem, M. A.; Pullen, S. S.; Takahashi, H. 5-Aminomethylbenzimidazoles as potent ITK antagonists. *Bioorg. Med. Chem. Lett.* **2009**, *19*, 1588–1591.

(20) Charrier, J. D.; Miller, A.; Kay, D. P.; Brenchley, G.; Twin, H. C.; Collier, P. N.; Ramaya, S.; Keily, S. B.; Durrant, S. J.; Knegetel, R. M.; Tanner, A. J.; Brown, K.; Curnock, A. P.; Jimenez, J. M. Discovery and structure-activity relationship of 3-aminopyrid-2-ones as potent and selective interleukin-2 inducible T-cell kinase (Itk) inhibitors. *J. Med. Chem.* **2011**, *54*, 2341–2350.

(21) Knegetel, R. M. A.; Robinson, D. D. A Role for Hydration in interleukin-2 inducible T cell kinase (Itk) selectivity. *Mol. Inf.* **2011**, *30*, 950–959.

(22) Flynn, G. A.; Lee, S. A.; Faris, M.; Brandt, D. W.; Chakravarty, S. Intracellular Kinase Inhibitors. US 2007/0293499 A1, 2007.

(23) Alder, C. M.; Baldwin, I. R.; Barton, N. P.; Campbell, A. J.; Champigny, A. C.; Harling, J. D.; Maxwell, A. C. Derivatives of 2-[2-(Benzo- or Pyrido-)thiazolylamino]-6-aminopyridine, Useful in the Treatment of Respiratory, Allergic or Inflammatory Diseases. WO 2011/110575 A1, 2011.

(24) Maxwell, A. C.; Alder, C.; Ambler, M.; Campbell, A.; Champigny, A.; Harling, J.; Scullion, C.; Smith, I.; Somers, D.; Tame, C.; Wilson, C.; Woolven, J. In *Identification of Novel and Selective ITK Inhibitors through a Template Hopping Strategy*; American Chemical Society: Washington, DC, 2011; pp MEDI-8.

(25) Cheng, Y.; Prusoff, W. H. Relationship between the inhibition constant (K_i) and the concentration of inhibitor which causes 50% inhibition (I₅₀) of an enzymatic reaction. *Biochem. Pharmacol.* **1973**, *22*, 3099–3108.

(26) Swinney, D. C. Biochemical mechanisms of drug action: what does it take for success? *Nat. Rev. Drug Discovery* **2004**, *3*, 801–808.

(27) Bogoyevitch, M. A.; Fairlie, D. P. A new paradigm for protein kinase inhibition: blocking phosphorylation without directly targeting ATP binding. *Drug Discovery Today* **2007**, *12*, 622–633.

(28) Harrison, S.; Das, K.; Karim, F.; Maclean, D.; Mendel, D. Non-ATP-competitive kinase inhibitors: enhancing selectivity through new inhibition strategies. *Expert Opin. Drug Discovery* **2008**, *3*, 761–774.

(29) Navratilova, I.; Macdonald, G.; Robinson, C.; Hughes, S.; Mathias, J.; Phillips, C.; Cook, A. Biosensor-based approach to the identification of protein kinase ligands with dual-site modes of action. *J. Biomol. Screening* **2012**, *17*, 183–193.

(30) Han, S. Unpublished results.

(31) Robertson, J. G. Mechanistic basis of enzyme-targeted drugs. *Biochemistry* **2005**, *44*, 5561–5571.

(32) Singh, J.; Petter, R. C.; Baillie, T. A.; Whitty, A. The resurgence of covalent drugs. *Nat. Rev. Drug Discovery* **2011**, *10*, 307–317.

(33) Schwobel, J. A.; Koleva, Y. K.; Enoch, S. J.; Bajot, F.; Hewitt, M.; Madden, J. C.; Roberts, D. W.; Schultz, T. W.; Cronin, M. T. Measurement and estimation of electrophilic reactivity for predictive toxicology. *Chem. Rev.* **2011**, *111*, 2562–2596.

(34) Kim, K. H.; Maderna, A.; Schnute, M. E.; Hegen, M.; Mohan, S.; Miyashiro, J.; Lin, L.; Li, E.; Keegan, S.; Lussier, J.; Wrocklage, C.; Nickerson-Nutter, C. L.; Wittwer, A. J.; Soutter, H.; Caspers, N.; Han, S.; Kurumbail, R.; Dunussi-Joannopoulos, K.; Douhan, J., 3rd; Wissner, A. Imidazo[1,5-a]quinoxalines as irreversible BTK inhibitors for the treatment of rheumatoid arthritis. *Bioorg. Med. Chem. Lett.* **2011**, *21*, 6258–6263.

(35) Pan, Z.; Scheerens, H.; Li, S. J.; Schultz, B. E.; Sprengeler, P. A.; Burrill, L. C.; Mendonca, R. V.; Sweeney, M. D.; Scott, K. C.; Grothaus, P. G.; Jeffery, D. A.; Spoerke, J. M.; Honigberg, L. A.; Young, P. R.; Dalrymple, S. A.; Palmer, J. T. Discovery of selective irreversible inhibitors for Bruton's tyrosine kinase. *ChemMedChem* **2007**, *2*, 58–61.

(36) Honigberg, L. A.; Smith, A. M.; Sirisawad, M.; Verner, E.; Loury, D.; Chang, B.; Li, S.; Pan, Z.; Thamm, D. H.; Miller, R. A.; Buggy, J. J. The Bruton tyrosine kinase inhibitor PCI-32765 blocks B-cell activation and is efficacious in models of autoimmune disease and B-cell malignancy. *Proc. Natl. Acad. Sci. U.S.A.* **2010**, *107*, 13075–13080.

(37) Wissner, A.; Mansour, T. S. The development of HKI-272 and related compounds for the treatment of cancer. *Arch. Pharm. (Weinheim, Ger.)* **2008**, *341*, 465–477.

(38) Nakayama, S.; Atsumi, R.; Takakusa, H.; Kobayashi, Y.; Kurihara, A.; Nagai, Y.; Nakai, D.; Okazaki, O. A zone classification system for risk assessment of idiosyncratic drug toxicity using daily dose and covalent binding. *Drug Metab. Dispos.* **2009**, *37*, 1970–1977.

(39) Please see Supporting Information for more details.

(40) Naramura, M.; Band, V.; Band, H. Indispensable roles of mammalian Cbl family proteins as negative regulators of protein tyrosine kinase signaling: Insights from in vivo models. *Commun. Integr. Biol.* **2011**, *4*, 159–162.

(41) Katkere, B.; Rosa, S.; Drake, J. R. The Syk-binding ubiquitin ligase c-Cbl mediates signaling-dependent B cell receptor ubiquitination and B cell receptor-mediated antigen processing and presentation. *J. Biol. Chem.* **2012**, *287*, 16636–16644.

(42) Paolino, M.; Thien, C. B.; Gruber, T.; Hinterleitner, R.; Baier, G.; Langdon, W. Y.; Penninger, J. M. Essential role of E3 ubiquitin ligase activity in Cbl-b-regulated T cell functions. *J. Immunol.* **2011**, *186*, 2138–2147.

(43) Compound 41 (PF-06465469) is now commercially available from Sigma-Aldrich Corp. (St. Louis, MO), Tocris Bioscience (Bristol, U.K.), or Toronto Research Chemicals, Inc. (North York, ON, Canada).

(44) Kawasaki, Y.; Freire, E. Finding a better path to drug selectivity. *Drug Discovery Today* **2011**, *16*, 985–990.

(45) Wang, Z.; Watt, W.; Brooks, N. A.; Harris, M. S.; Urban, J.; Boatman, D.; McMillan, M.; Kahn, M.; Heinrikson, R. L.; Finzel, B. C.; Wittwer, A. J.; Blinn, J.; Kamtekar, S.; Tomasselli, A. G. Kinetic and structural characterization of caspase-3 and caspase-8 inhibition by a

novel class of irreversible inhibitors. *Biochim. Biophys. Acta* **2010**, *1804*, 1817–1831.

(46) Singh, J.; Dobrusin, E. M.; Fry, D. W.; Haske, T.; Whitty, A.; McNamara, D. J. Structure-based design of a potent, selective, and irreversible inhibitor of the catalytic domain of the erbB receptor subfamily of protein tyrosine kinases. *J. Med. Chem.* **1997**, *40*, 1130–1135.